Spring 5-31-1974

A nonlinear viscoelastic model

Yon-Li Shangkuan
New Jersey Institute of Technology

Copyright Warning & Restrictions

The copyright law of the United States (Title 17, United States Code) governs the making of photocopies or other reproductions of copyrighted material.

Under certain conditions specified in the law, libraries and archives are authorized to furnish a photocopy or other reproduction. One of these specified conditions is that the photocopy or reproduction is not to be "used for any purpose other than private study, scholarship, or research." If a, user makes a request for, or later uses, a photocopy or reproduction for purposes in excess of "fair use" that user may be liable for copyright infringement,

This institution reserves the right to refuse to accept a copying order if, in its judgment, fulfillment of the order would involve violation of copyright law.

Please Note: The author retains the copyright while the New Jersey Institute of Technology reserves the right to distribute this thesis or dissertation

Printing note: If you do not wish to print this page, then select "Pages from: first page # to: last page #" on the print dialog screen

A NONLINEAR VISCOELASTIC MODEL

BY

YON-LI SHANGKUAN

A DISSERTATION

PRESENTED IN PARTIAL FULFILLMENT OF

THE REQUIREMENTS FOR THE DEGREE

OF

DOCTOR OF ENGINEERING SCIENCE

AT

NEWARK COLLEGE OF ENGINEERING

Newark, New Jersey

1974

ABSTRACT

A nonlinear viscoelastic model has been developed to describe the non-Newtonian viscosities and the primary normal stress differences of high polymers at steady-state shearing flow.

It has been demonstrated that the Huang-Shangkuan model gives the best representation of the experimental data for a wide range of shear rates. In the high shear rate region the Huang-Shangkuan model is distinguished among other models by its capability to predict the non-Newtonian viscosities and the primary normal stress differences which the other models fail to predict.

Continuum mechanics, Lodge's network theory and Rouse's theory provide specific information in developing our model. The theoretical aspect of this model is also supported by the experimental data, which were taken using the accurate Weissenberg rheogoniometer.

APPROVAL OF DISSERTATION

A NONLINEAR VISCOELASTIC MODEL

BY

YON-LI SHANGKUAN

FOR

DEPARTMENT OF CHEMICAL ENGINEERING

NEWARK COLLEGE OF ENGINEERING

BY

FACULTY COMMITTEE

APPROVED:

NEWARK, NEW JERSEY

MAY, 1974

ACKNOWLEDGEMENT

The author is much indebted to Dr. Ching-Rong Huang, thesis advisor, under whose guidance this research was performed. In addition, he inculcated in the author a special interest in the field of rheology.

The author wishes to express his appreciation to Dr. W. Philippoff for his kind preparation of test samples. The author acknowledges the assistance given to him by Dr. N. Siskovic in the experimental aspect of this work. I express my sincere gratitude to my wife, Pei-Wha, for her inspiration, encouragement and patience during my work.

The author acknowledges financial support offered by the Research Foundation of Newark College of Engineering.

TABLE OF CONTENTS

LIST OF TABLES AND FIGURES

PAGE

TABLE

FIGURE

PAGE

CHAPTER 1 INTRODUCTION

(1.1) General Description

Most fluids of industrial importance are characterized by the well-known Newtonian hypothesis (5), in which the shear stress is proportional to the shear rate. However, for liquids or solutions of very high molecular weight (say, M.W. $> 10^4$) striking deviations from the above hypotheses are obviously observed. Similarly other structurally complex materials, such as liquid crystals, soap solutions and pastes, deviate from Newtonian behavior. All these fluids are referred to as "non-Newtonian fluids".

Classification of Fluids

(1.2) Viscous Fluids—Newtonian Fluids

The stress-deformation behavior of this ideal body is best considered by imagining two parallel plates of very large area (A) separated a very small distance r by the viscous fluid. A shear force $\mathcal{F}$ is applied to the top plate and the top plate is moving with a constant velocity V along the x-direction (Fig. 1-1).

Fluids which obey the following simple relations

$$\mathcal{F} = -\mu \left(\frac{d v_x}{d y}\right) = \mu \dot{\gamma} \qquad (1-1)$$

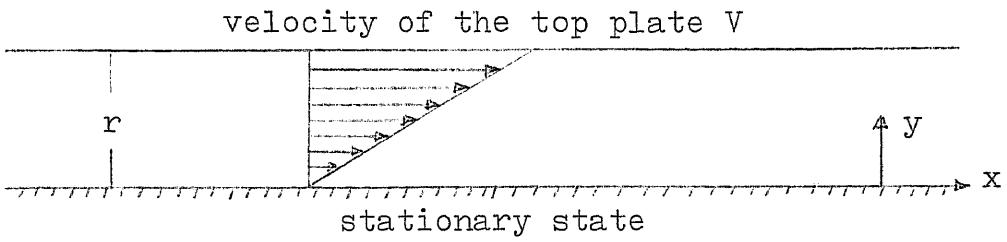

Fig. 1-1 Shear Deformation

where the constant μ is known as the coefficient of viscosity are referred to as Newtonian fluids. In eq. (1-1) $\dot{\gamma} = -dv_x/dy$ is defined as the shear rate.

(1.3) Non-Newtonian Fluids

Non-Newtonian fluids can also be classified into three broad classes of flow behavior (10); time-dependent, time-independent and viscoelastic fluids.

(a) time-independent fluids

Fluids in which the shear stress is a function of the shear rate only are defined mathematically by the equation

$$\tau = \eta \left(\frac{-dv_x}{dy} \right) = \eta \dot{\gamma} \qquad (1\text{-}2)$$

where η defined as the non-Newtonian viscosity is a function of $\dot{\gamma}$.

(b) time-dependent fluids

Fluids are those in which the shear stress is a function of both the shear rate and time. These fluids are

expressed by

$$\tau = f(\dot{\gamma}, t) \qquad (1\text{-}3)$$

There are three kinds of time-dependent fluids: thixotropic, anti-thixotropic and rheopectic (50).

(c) viscoelastic fluids

Viscoelastic fluids are those which are predominantly viscous but which exhibit partial elastic recovery after deformation. One simple form in representing the viscous and elastic properties of fluids is

$$\eta = f(\dot{\gamma}, \tau, \dot{\tau}) \qquad (1\text{-}4)$$

where $\dot{\tau}$ is the rate of shear stress*.

The viscoelastic property of fluids manifests itself in such phenomena as die swell and calender swell in industrial processing. Examples of economically important uses of viscoelastic fluids are to be found in the plastics industry and in the production of synthetic fibres, in oil well technology (drilling fluids), in biology, in rocket fuels and in the application of coatings. (See the August 1964 issue of Chemical Engineering Progress.)

(1.4) Failure of Previous Viscoelastic Models

In the recent years, many attempts have been made to

---

* The detailed mathematical description is in chapter 3.

derive rheological equations which could describe viscoelastic behavior. Unfortunately it is commonly found that most derived equations could not predict experimental observations, particularly those at high shear rates (8)(9)(42) except occasionally in simple steady flow situations where elastic effects are assumed negligible. On the other hand linear viscoelastic models and molecular theories in general are restricted to very small rates of shear flow or cannot show a nonlinear viscoelastic behavior at large rates of shear.

The most successful models in the past come from the nonlinear extensions of the differential or integral equations from generalized Maxwell equations or from Lodge's network theory (29)(50). For example, the models such as the Spriggs and WJFLMB models (25)(27)(42)(47) are shown to describe qualitatively all viscoelastic properties with rate-of-shear dependence. The Bird-Carreau model is able to predict the behavior of a large variety of fluids at low range of shear rates. However it fails to describe rheological properties of some polymer solutions under a steady state when the shear rate becomes quite high (6)(12).

(1.5) The Purpose of This Thesis

The main purpose of this work is to obtain a realistic rheological model which not only is free of the weak points of previous models but also describes reasonably the behav-

ior of polymer solutions for a wide range of shear rates. Whenever possible, information from molecular theories will be used to interpret the physical meanings of parameters in our model.

CHAPTER 2 TENSOR APPLICATION TO RHEOLOGICAL EQUATIONS

(2.1) Introduction

Generally speaking, the rheological equations defining the properties of an element of a viscoelastic fluid may involve all the kinematic and dynamic quantities. The form of the completely general rheological equations should be restricted by the requirement that the equations describe rheological properties independent of the coordinate systems. In order to describe the motion of a continuous media, it is inconvenient to use a fixed set of coordinates. Instead, a convected (moving) frame of reference is needed in connection with the description of the deformations of fluids. In the present chapter, tensor methods for describing finite deformations of fluids are applied to the development of rheological equations.

(2.2) Convected and Space-Fixed Systems

The motion of fluid can be described mathematically by (29)

$$x^{i} = f^{i}(\xi, t) , \qquad \xi^{i} = \phi^{i}(x, t) \tag{2-1}$$

where x^i is the fixed space coordinate of space points at an instant time t; ξ^i is the convected body coordinate of a particle in space at an instant time t. In the above

equation, x stands for a set of coordinates x^1, x^2, x^3 and ξ for a set of coordinates ξ^1, ξ^2, ξ^3. We may assign numbers to the convected coordinates of the particle at some reference time t_0.

(2.3) Base Vectors, Metric Tensors, Displacement Tensors and Deformation Tensors

Given a position vector $\underline{r}$ in a fixed coordinate system we have (40)(41)

$$d\underline{r} = \frac{\partial \underline{r}}{\partial x^1} dx^1 + \frac{\partial \underline{r}}{\partial x^2} dx^2 + \frac{\partial \underline{r}}{\partial x^3} dx^3$$

$$= \sum_{i=1}^{3} \frac{\partial \underline{r}}{\partial x^i} dx^i \qquad (2\text{-}2)$$

In a shorter notation eq. (2-2) can be written as

$$d\underline{r} = \frac{\partial \underline{r}}{\partial x^i} dx^i \qquad (2\text{-}3)$$

then

$$ds^2 = d\underline{r} \cdot d\underline{r} = \frac{\partial \underline{r}}{\partial x^i} dx^i \cdot \frac{\partial \underline{r}}{\partial x^j} dx^j$$

$$= \frac{\partial \underline{r}}{\partial x^i} \cdot \frac{\partial \underline{r}}{\partial x^j} dx^i dx^j \qquad (2\text{-}4)$$

where $\frac{\partial \underline{r}}{\partial x^i} \cdot \frac{\partial \underline{r}}{\partial x^j}$ is defined as $g_i \cdot g_j$ (g_{ij}). The quantities $\underline{g}_i$ are defined as a covariant base vector and g_{ij} as a covariant metric tensor. Similarly contravariant base vectors can be defined as the solutions of

$$\underline{g}^i \cdot \underline{g}_j = \delta^i_j$$

where δ^i_j is a Kronecker delta.

Contravariant metric tensors are given by

$$g^{ij} = \underline{g}^i \cdot \underline{g}^j \tag{2-5}$$

In the convected system base vectors and metric tensors can be defined in the same way as those in the fixed coordinate system. Namely

$$\hat{\underline{g}}_\alpha(\xi, t) = \frac{\partial \underline{r}(\xi, t)}{\partial \xi^\alpha} \tag{2-6}$$

$$\hat{\underline{g}}^\alpha(\xi, t) \cdot \hat{\underline{g}}_\beta(\xi, t) = \delta^\alpha_\beta \tag{2-7}$$

$$\hat{\underline{g}}^\alpha(\xi, t) \cdot \hat{\underline{g}}^\beta(\xi, t) = \hat{g}^{\alpha\beta}(\xi, t) \tag{2-8}$$

$$\hat{\underline{g}}_\alpha(\xi, t) \cdot \hat{\underline{g}}_\beta(\xi, t) = \hat{g}_{\alpha\beta}(\xi, t) \tag{2-9}$$

where $\hat{\underline{g}}_\alpha(\xi, t)$: convected covariant base vector

$\hat{\underline{g}}^\alpha(\xi, t)$: convected contravariant base vector

$\hat{g}^{\alpha\beta}(\xi, t)$: convected contravariant metric tensor

$\hat{g}_{\alpha\beta}(\xi, t)$: convected covariant metric tensor

The convected base vectors or metric tensors can be related in the same manner as two sets of base vectors or metric tensors are related in classical vector and tensor analysis (52). Thus we have

$$\hat{\underline{g}}_\alpha = \frac{\partial \underline{r}}{\partial \xi^\alpha} = \frac{\partial \underline{r}}{\partial x^i} \frac{\partial x^i}{\partial \xi^\alpha} = \frac{\partial x^i}{\partial \xi^\alpha} \underline{g}_i \tag{2-10}$$

and

$$\hat{\underline{g}}^\alpha = \frac{\partial \xi^\alpha}{\partial x^i} \underline{g}^i \tag{2-11}$$

where x^i and ξ^α are related by eq. (2-1).

From Noll's terminology (33) one may define a displacement tensor $\underline{\underline{F}}$ and its inverse $\underline{\underline{F}}^{-1}$ for the purpose of describing deformation tensors which are extensively applied to the building of nonlinear viscoelastic models (2)(3)(4)(13)(25)(27)(29)(44). The representations for F and F^{-1} are

$$\underline{\underline{F}} = \hat{\underline{g}}_\alpha(\xi,t)\,\underline{g}^\alpha(X_0) = \underline{\hat{g}}_\alpha(\xi,t)\,\hat{\underline{g}}^\alpha(\xi,t_0) \qquad (2\text{-}12\text{-}A)$$

$$\underline{\underline{F}}^{-1} = \hat{\underline{g}}_\alpha(X_0)\,\hat{\underline{g}}^\alpha(\xi,t) = \hat{\underline{g}}_\alpha(\xi,t_0)\,\hat{\underline{g}}^\alpha(\xi,t) \qquad (2\text{-}12\text{-}B)$$

$\underline{\underline{F}}$ and $\underline{\underline{F}}^{-1}$ defined in above two equations are satisfied by:

$$\hat{\underline{g}}_\alpha(\xi,t) = \underline{\underline{F}} \cdot \underline{g}_\alpha(X_0) \qquad (2\text{-}13)$$

$$\hat{\underline{g}}^\alpha(\xi,t) = \underline{g}^\alpha(X_0) \cdot \underline{\underline{F}}^{-1} \qquad (2\text{-}14)$$

$$\underline{g}_\alpha(X_0) = \underline{\underline{F}}^{-1} \cdot \hat{\underline{g}}_\alpha(\xi,t) \qquad (2\text{-}15)$$

$$\underline{g}^\alpha(X_0) = \underline{\underline{F}} \cdot \hat{\underline{g}}^\alpha(\xi,t) \qquad (2\text{-}16)$$

$$\underline{\underline{F}} \cdot \underline{\underline{F}}^{-1} = \underline{\underline{F}}^{-1} \cdot \underline{\underline{F}} = \underline{\underline{\delta}} \qquad (2\text{-}17)$$

where $\underline{\underline{\delta}}$ is the unit tensor. In eq.(2-13) the tensor $\underline{\underline{F}}$ transforms the covariant base vector associated with a given particle at time t_0 into the convected covariant base vector associated with the same particle at time t. The functions of $\underline{\underline{F}}$ or $\underline{\underline{F}}^{-1}$ in eqs. (2-14),(2-15),(2-16) could be explained similarly as that in eq. (2-13). The transposes of $\underline{\underline{F}}$ and $\underline{\underline{F}}^{-1}$ could be written as

$$\underline{\underline{F}}^T = \underline{g}^\alpha(X_0)\,\hat{\underline{g}}_\alpha(\xi,t) = \hat{\underline{g}}^\alpha(\xi,t_0)\,\hat{\underline{g}}_\alpha(\xi,t) \qquad (2\text{-}18)$$

$$\underline{\underline{F}}^{-1T} = \hat{\underline{g}}^{\alpha}(\xi,t)\,\underline{g}_{\alpha}(X_0) = \hat{\underline{g}}^{\alpha}(\xi,t)\,\hat{\underline{g}}_{\alpha}(\xi,t_0) \qquad (2\text{-}19)$$

In terms of displacement tensors one can now define deformation tensors such as the Cauchy tensor, the Finger tensor, the Green tensor and the Piola tensor as follows (18)

$$\underline{\underline{C}}(t,t_0) = \underline{\underline{F}}^{-1T}\cdot\underline{\underline{F}}^{-1} = \hat{g}_{\alpha\beta}(\xi,t_0)\,\hat{\underline{g}}^{\alpha}(\xi,t)\,\hat{\underline{g}}^{\beta}(\xi,t)$$

(Cauchy) (2-20)

$$\underline{\underline{C}}^{-1}(t,t_0) = \underline{\underline{F}}\cdot\underline{\underline{F}}^{T} = \hat{g}^{\alpha\beta}(\xi,t_0)\,\hat{\underline{g}}_{\alpha}(\xi,t)\,\hat{\underline{g}}_{\beta}(\xi,t)$$

(Finger) (2-21)

$$\underline{\underline{C}}(t_0,t) = \underline{\underline{F}}^{T}\cdot\underline{\underline{F}} = \hat{g}_{\alpha\beta}(\xi,t)\,\hat{\underline{g}}^{\alpha}(\xi,t_0)\,\hat{\underline{g}}^{\beta}(\xi,t_0)$$

(Green) (2-22)

$$\underline{\underline{C}}^{-1}(t_0,t) = \underline{\underline{F}}^{-1}\cdot\underline{\underline{F}}^{-1T} = \hat{g}^{\alpha\beta}(\xi,t)\,\hat{\underline{g}}_{\alpha}(\xi,t_0)\,\hat{\underline{g}}_{\beta}(\xi,t_0)$$

(Piola) (2-23)

The notation above displays explicitly the relations among the four tensors. For example, if the reference state t_0 and the present state t are interchanged (i.e. $t_0 \rightarrow t$), then the Green tensor becomes the Cauchy tensor. Through the transformation rules of tensors (32)(36), the above equations can be written in a fixed-coordinate system.

$$\underline{\underline{C}}(t,t_0) = g_{\alpha\beta}(X_0)\,\frac{\partial\xi^{\alpha}}{\partial X^{i}}\,\frac{\partial\xi^{\beta}}{\partial X^{j}}\,\underline{g}^{i}(X)\,\underline{g}^{j}(X)$$

(Cauchy) (2-24)

$$\underline{\underline{C}}^{-1}(t,t_0) = g^{\alpha\beta}(X_0)\frac{\partial X^i}{\partial \xi^\alpha}\frac{\partial X^j}{\partial \xi^\beta}\underline{g}_i(X)\underline{g}_j(X)$$

(Finger) (2-25)

$$\underline{\underline{C}}(t_0,t) = g_{\alpha\beta}(X)\frac{\partial X^\alpha}{\partial \xi^i}\frac{\partial X^\beta}{\partial \xi^j}\underline{g}^i(X_0)\underline{g}^j(X_0)$$

(Green) (2-26)

$$\underline{\underline{C}}(t_0,t) = g^{\alpha\beta}(X)\frac{\partial \xi^i}{\partial X^\alpha}\frac{\partial \xi^j}{\partial X^\beta}\underline{g}_i(X_0)\underline{g}_j(X_0)$$

(Piola) (2-27)

The Cauchy, Finger, Green or Piola tensors with their derivatives* are usually starting points for modifying the small rate of the deformation tensor $\dot{\gamma}_{ij}$ in the generalized Maxwell model, in order to obtain a reasonable rheological model which could predict the Weissenberg effects of elastic effects of polymers at large rates of deformation (6)(12) (31)(32).

---

* For details of derivatives of these tensors, refer to reference (18).

CHAPTER 3 NONLINEAR VISCOELASTIC MODEL BUILDING

(3.1) Introduction

The response of a material to an applied stress can, in principle, be predicted if the rheological equation of the material is known. During the past two decades, much effort has been put into developing rheological models in order to predict the rheological properties such as non-Newtonian viscosities, normal stress differences, etc.. It would be most satisfying to be able to develop everything and to predict experimental observations with a nonlinear equation from a molecular point of view. However due to complex physical phenomena of high polymers at large rates of deformation (7)(14), successful molecular theories to rheological model building in general are restricted to very small rates of deformation*. Therefore several research groups have put much effort into developing nonlinear rheological equations only from the phenomenological point of view (24). In the phenomenological approach, emphasis is put on formulating the relationship between the components of stresses (shear stress or normal stress) and the rate of deformation. The parameters involved in a rheological model presumably represent the characteristics of the material. Whenever possible, information from the mo-

* Sec. (1.5) in chapter 1.

lecular theories will be applied to explain the flow properties. There are two general approaches toward nonlinear viscoelastic model building. These will be discussed as follows.

(3.2) Generalized Maxwell Model

The simple Maxwell element* is made up of combinations of spring and dash-pot. One can regard the force on a spring as proportional to strain and the force on a dash-pot as proportional to the rate of strain. Consequently the spring and dash-pot represent the elastic and viscous properties of the fluid respectively. The equation is

$$\tau_{ij} + \frac{\eta}{G}\frac{\partial \tau_{ij}}{\partial t} = -\eta \dot{\gamma}_{ij} \qquad (3\text{-}1)$$

in which η is the viscosity and G is the rigidity.

Fig. 3-1 Maxwell Body

* Refer to Fig. 3-1.

In eq. (3-1) $\frac{\eta}{G}$ is defined as the relaxation time (7). The simple Maxwell body cannot describe normal stress difference or non-Newtonian viscosity of real viscoelastic liquids adequately in most cases, but it could be generalized by the idea that the total stress in the liquids is the superposition of individual stress, each arising from the motion of molecular segments of various sizes (32). Therefore

$$\tau_{ij} = \sum_{p=1}^{\infty} \tau_{ij}^{(p)} \qquad (3\text{-}2\text{-}A)$$

$$\left(1 + \lambda_p \frac{\partial}{\partial t}\right) \tau_{ij}^{(p)} = -\eta_p \dot{\gamma}_{ij} \qquad (3\text{-}2\text{-}B)$$

Eqs. (3-2-A) and (3-2-B) can be written in three other equivalent forms as (7)

$$\left(1 + \sum_{p=1}^{\infty} a_n \frac{\partial^n}{\partial t^n}\right) \tau_{ij} = -\eta_0 \left(1 + \sum_{p=1}^{\infty} b_n \frac{\partial^n}{\partial t^n}\right) \dot{\gamma}_{ij} \qquad (3\text{-}3)$$

$$\tau_{ij} = -\int_{-\infty}^{t} \left\{ \sum_{p=1}^{\infty} \frac{\eta_p}{\lambda_p} e^{-\frac{(t-t')}{\lambda_p}} \right\} \dot{\gamma}_{ij}(t')\, dt' \qquad (3\text{-}4)$$

"relaxation function"

$$\tau_{ij} = \int_{-\infty}^{t} \left\{ \sum_{p=1}^{\infty} \frac{\eta_p}{\lambda_p^2} e^{-\frac{(t-t')}{\lambda_p}} \right\} \dot{\gamma}_{ij}(t')\, dt' \qquad (3\text{-}5)$$

"memory function"

Eqs. (3-2) and (3-3) are the differential forms of the generalized Maxwell model. In eq. (3-5) $\gamma_{ij}(t')$ is defined as an infinitesimal strain tensor* ($\underline{\gamma} = \nabla\underline{U} + (\nabla\underline{U})^+$) where $\underline{U}$ is the displacement vector (6)(36); the last two equations are the integral forms in which the present time t is taken as the reference state to which the states of the fluid at past time t' are referred. Generally speaking, the description of rheological properties of material at small rates of deformation (i.e. linear viscoelasticity) can be made quite satisfactorily with any of above four equations (5). However in an attempt to predict rheological behavior at large rates of deformation, the generalized Maxwell model must be modified. A brief listing of the modified models stemming from the above four forms can be written as follows.

models based on equation	models
(3-2)	Spriggs (44), White-Metzner (48)
(3-3)	Oldrolyd (34), Roscoe (38)
(3-4)	Walters (47), Fredrickson (21)
(3-5)	WJFLMB (42), Bird-Carreau (6)(12)

It is understood that the principle of material objectivity must be satisfied, when making modifications of the

---

* $(\nabla\underline{U})^+$ is the transpose of $\nabla\underline{U}$.

generalized Maxwell model, so that invariance properties are not changed (29)(6)(12)(33)(36). The principle of material objectivity states that the form of any rheological equations must be the same in any two coordinate system; for example finite strain tensors (the Finger tensor etc.) and their derivatives with respect to time satisfy rules of tensor transformation in both convected and fixed coordinate systems. The generalized Maxwell model as mentioned satisfies the principle of material objectivity only under a very small rate of deformation.

(3.3) Functional Analysis

The functional approach has been used to obtain various rheological models by Lodge (29), Coleman and Noll (15). The definition of a functional is: a variable y is said to be a functional of x(t) if the value of y is determined by the value of x(t') throughout the interval $t_0 \leq t' \leq t$. The mathematical form is

$$y = \mathcal{F}\left\{ \overset{t}{\underset{t_0}{x}}(t') \right\} \tag{3-6}$$

One of the familiar examples in eq. (3-6) is the integration of x(t') from t_0 to t

$$y = \int_{t_0}^{t} x(t')\,dt' \tag{3-7}$$

A more general form of the above equation still linear in x(t) is

$$y_1 = \int_{t_0}^{t} K_1(t;t')\, x(t')\, dt' \qquad (3\text{-}8)$$

in which $K_1(t;t')$ is defined as the kernel.

There is a fundamental theorem in the calculus of functionals (29)(46), which states that y can be expressed as a series of integrals. Therefore

$$y_1 = y_1 + y_2 + y_3 + \text{- - - -} \qquad (3\text{-}9)$$

where y_1 is expressed in eq. (3-8) and

$$y_2 = \int_{t_0}^{t}\int_{t_0}^{t} K_2(t;t',t'')\, x(t')\, x(t'')\, dt'\, dt'' \qquad (3\text{-}10)$$

This process of generalization can be continued to obtain the triple integral in y_3 etc.. We may therefore follow the same fashion in eq. (3-6) and express the contravariant stress as

$$\mathcal{T}^{ij} = \mathcal{F}^{ij}\left\{ \overset{t}{\underset{-\infty}{\hat{g}^{kl}}}(t') \right\} \qquad (3\text{-}11)$$

where $\hat{g}^{kl}(t')$ is the convected contravariant metric tensor as seen in eq. (2-8). The range of the variable t' is extended to $-\infty$ on the assupmtion that the stress at any time t in an element of material is determined by the flow history of the shape of that element. The expansion of eq. (3-11) by the use of eq. (3-9) results in

$$\tau^{ij} = \mathcal{F}_{(1)}^{ij} + \mathcal{F}_{(2)}^{ij} + \mathcal{F}_{(3)}^{ij} + \cdots\cdots \qquad (3\text{-}12)$$

where

$$\mathcal{F}_{(1)}^{ij} = \int_{-\infty}^{t} K_1(t;t')\, \hat{g}^{ij}(t')\, dt' \qquad (3\text{-}13)$$

The form of $\mathcal{F}_{(2)}^{ij}$ and higher terms in eq. (3-12) is much more complicated because $\hat{g}^{ij}(t')$, $\hat{g}^{ij}(t'')$ must satisfy the principle of material objectivity. One possible combination is (29)

$$\int_{-\infty}^{t}\int_{-\infty}^{t} K_2(t;t',t'')\, \hat{g}_{rs}(t)\, \hat{g}^{ri}(t')\, \hat{g}^{sj}(t'')\, dt'dt'' \qquad (3\text{-}14)$$

Similarly the contravariant stress tensor can be expressed by

$$\tau_{ij} = \mathcal{F}_{ij}\left\{ \hat{g}_{kl}^{\,t}(t') \right\}_{-\infty} \qquad (3\text{-}15)$$

where τ_{ij} is the covariant stress tensor

$\hat{g}_{kl}(t)$ is the convected covariant metric tensor

For the form in eq. (3-15), Coleman and Noll have shown that the application of functional analysis and the principle of material objectivity lead to the following rheological equation expressed in the fixed-coordinate system (16)

$$\gamma_{ij} = -\int_{-\infty}^{t} \mu_1(t-t')\,\Gamma_{ij}(t')\,dt' - \int_{-\infty}^{t}\int_{-\infty}^{t} \left[\mu_2(t-t',t'')\,\Gamma_{ik}(t')\,\Gamma_{j}^{k}(t'')\right.$$

$$\left. + \mu_3(t-t',t'')\,\Gamma_{k}^{k}(t')\,\Gamma_{ij}(t'')\right] dt'\,dt'' \qquad (3\text{-}16)$$

where

$$\Gamma_{ij}(t') = g_{ij}(x) - C_{ij}(t,t') \qquad (3\text{-}17)$$

and $C_{ij}(t,t")$ is the Cauchy tensor given in eq. (2-24). μ_1, μ_2, μ_3 are unspecified memory functions. In eqs. (3-16), and (3-17), $g_{ij}(x)$ are the covariant components of the fixed metric tensor. It is interesting to note that the general equation (3-16) reduces after simplification to some equivalent viscoelastic models, which extend from the generalized Maxwell equation (14).

CHAPTER 4 SOME PHENOMENA OF POLYMERIC FLUIDS

(4.1) Steady-State Shearing Flow

Consider a fluid placed between two parallel plates as shown in Fig. 1-1 in which there exists a non-zero component of velocity in only the x-direction. If the subscripts x,y,z denote, respectively, the flow direction, the direction of velocity variation, and the neutral direction, then the flow is defined as the steady-state shearing flow*; that is

$$\underline{v} = (v_x, 0, 0) \tag{4-1}$$

$$\underline{\underline{\Delta}} = \frac{-dv_x}{dy}\begin{pmatrix} 0 & 1 & 0 \\ 1 & 0 & 0 \\ 0 & 0 & 0 \end{pmatrix} = -\dot{\gamma}_{xy}\begin{pmatrix} 0 & 1 & 0 \\ 1 & 0 & 0 \\ 0 & 0 & 0 \end{pmatrix}$$

$$= \dot{\gamma}\begin{pmatrix} 0 & 1 & 0 \\ 1 & 0 & 0 \\ 0 & 0 & 0 \end{pmatrix} \tag{4-2}$$

---

* For detailed definitions of this type of flow, see ref. (29).

where $\dot{\gamma}$ is the magnitude of the rate of deformation tensor $\underline{\underline{\dot{e}}}^*$ and is usually called the "shear rate" (p. 4 ref. 7 and p. 8 ref. 32). Shear stresses $\mathcal{T}_{xy}$ and normal-stress differences, which exist in steady-state shearing flow, are among the most commonly measured rheological properties of viscoelastic fluids. They are very important in engineering problems involving the flow of polymer solutions or polymer melts. Hence, any adequate rheological model must have a good description of the rate-of-shear dependence of the non-Newtonian viscosities and normal stress differences. The simple steady-state shearing flow can also exist in other flow geometries such as cone and plate flow, cylindrical flow (Poiseuille flow), Couette flow etc..

(4.2) Definition of the Coefficient of Normal-Stress Difference

The coefficients of the normal-stress difference in polymeric fluids are defined as

$$\theta = -(\mathcal{T}_{xx} - \mathcal{T}_{yy}) / \dot{\gamma}_{yx}^2 \qquad (4\text{-}3)$$

$$\zeta = -(\mathcal{T}_{xx} - \mathcal{T}_{zz}) / \dot{\gamma}_{yx}^2 \qquad (4\text{-}4)$$

$$\beta = -(\mathcal{T}_{yy} - \mathcal{T}_{zz}) / \dot{\gamma}_{yx}^2 \qquad (4\text{-}5)$$

---

* $\dot{e}_{yx}$ is the yx-component of the rate of deformation tensor $\underline{\underline{\dot{e}}} = (\nabla \underline{v} + \nabla \underline{v}^+)$ where + indicates the transpose. The quantity $\dot{\gamma}$ is the magnitude of $\underline{\underline{\dot{e}}}$ defined by $\dot{\gamma} = \sqrt{\frac{1}{2}(\underline{\underline{\dot{e}}} : \underline{\underline{\dot{e}}})}$ $= \sqrt{\frac{1}{2}\sum_i\sum_j \dot{e}_{ij}^2}$. In steady-state shearing flow $\dot{\gamma} = |\dot{e}_{xy}| = |\dot{\gamma}_{xy}|$ where $\dot{\gamma}_{xy}$ is defined as $-dv_x/dy$.

where θ , ξ and β (only two of which are independent) are functions of $\dot{\gamma}_{yx}$; θ is the primary normal-stress coefficient and β is the secondary normal-stress coefficient. The definitions of θ , ξ , β are taken in eqs. (4-3)(4-4)(4-5) because many fluids exhibit a quadratic dependence of normal stress differences on shear rate in the limit of shear rate (p. 10 ref. 32). For some time it is thought that $\tau_{yy} = \tau_{zz}$ (or $\beta = 0$) and this relation is called the Weissenberg hypothesis. The normal stress differences do not exist for Newtonian fluids; therefore, $\theta = \xi = \beta = 0$.

(4.3) Some Illustrations of the Normal-Stress Effects of Polymeric Materials

In order to illustrate the main differences between the behavior of Newtonian and non-Newtonian fluids, the following experiments were proposed (7)(29). The Newtonian

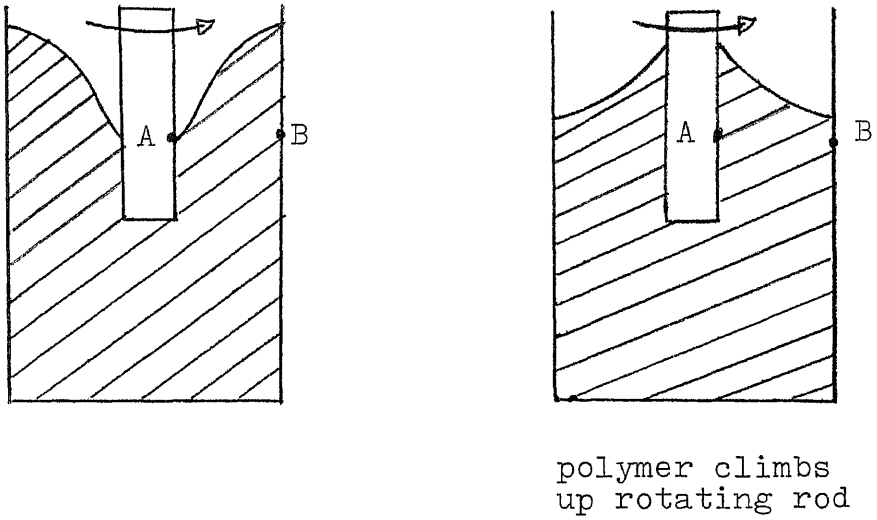

Fig. 4-1 Climbing Effect of Non-Newtonian Behavior

fluid is indicated on the left and the polymeric material on the right in each figure.

In Fig. 4-1 is an observation of the shape of the surface of a fluid in a beaker, into which a rotating rod is inserted. The Newtonian fluid on the left graph is moving toward the wall of the beaker because of the centrifugal force; the polymeric fluid placed on the right beaker moves toward the rotating rod and climbs up the rod due to normal stress effect. This phenomenon is called the Weissenberg effect which has been fully explained by Weissenberg himself (29).

An additional measurement can be made by putting pressure taps at A and B. For the Newtonian fluids the pressure at B exceeds that at A because of centrifugal force; on the other hand the pressure at A exceeds that at B for non-Newtonian fluids.

When a solution of a polymer of sufficiently high molecular weight flows out of a tube, the diameter of the emerging liquid increases; this is named the die swell effect of polymers shown in Fig. 4-2, which has been observed very often in many industrial operations. However, for the Newtonian fluids, the diameter of the emerging fluids is reduced by 13% because of a consideration of momentum conservation (29).

In Fig. 4-3 is the axial laminar flow in a concentric annulus (28). The pressure taps are mounted on either

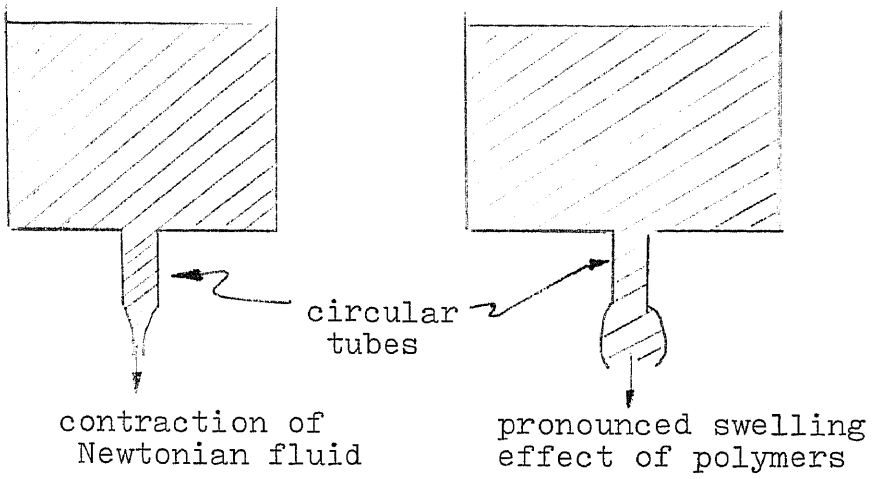

Fig. 4-2 Die Swell Effect

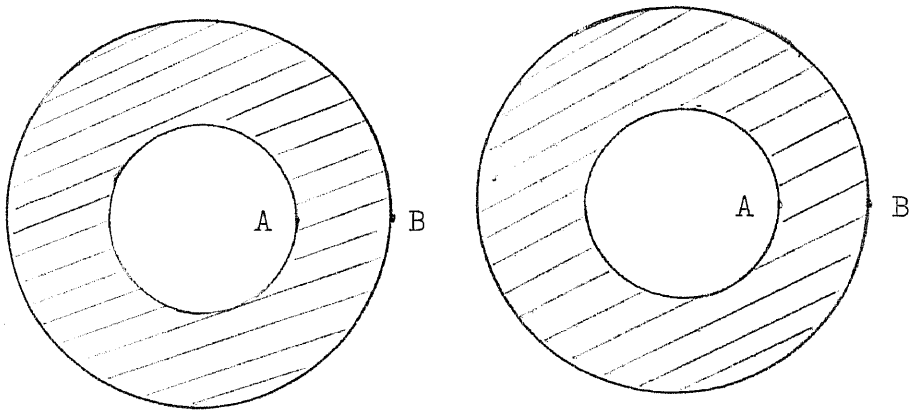

Fig. 4-3 Pressure Difference in the Axial Laminar Flow

side of the annular gap at the same height. For Newtonian fluids, pressure readings at A and B are the same; on the other hand, the pressure reading at A is greater than that at B for the non-Newtonian fluids.

(4.4) Summary

From above illustrations one comes to the conclusion that at steady-state shearing flow the polymeric fluids and Newtonian fluids have striking differences in behavior due to normal stress effects. Since 1950 normal stresses have been studied by phenomenological approach with extensive experimental observations. However molecular theories developed so far to explain the complicated phenomena in polymeric fluids are still not satisfactory. The presently available molecular theories in the literature seem to fall into three main categories:

(a) Bead-spring theories appropriate for dilute macromolecular solutions (38)(54).

(b) Chain-chain interaction theories, appropriate for solutions of intermediate concentrations.

(c) Network theories, appropriate for concentrated solutions and melts (29)(53).

CHAPTER 5 A PROPOSED RHEOLOGICAL MODEL

(5.1) Types of Rheological Models

In the past two decades we have seen that for the steady state shearing flow at small rates of deformation the generalized Maxwell model could provide an adequate description of rheological behavior of dilute polymer solutions. However, when the rates of deformation become large, any one of the four forms of the generalized Maxwell equation given in eqs. (3-2-A) to (3-5) fails to predict the rheological properties. The types of rheological models can be classified as

(a) linear viscoelastic models

The differential forms or integral forms of the generalized Maxwell model fall into this category; they are written in fixed coordinates for the infinitesimal strain γ or the infinitesimal rate of strain $\dot{\gamma}$.

(b) nonlinear viscoelastic models

In attempting to develop these nonlinear models, most investigators have chosen to begin with any one of the generalized Maxwell model and modify it in various ways to make the equation capable of describing some large deformation phenomena. From continuum mechanics we have the requirement of material objectivity. This means that an acceptable rheological equation should be independent of rigid

body motions; in other words, the form of any rheological equation must be the same in any two coordinate systems. If one uses convected coordinates correctly in formulating rheological equations, this requirement is satisfied automatically (36). For example, the Spriggs model is a nonlinear differential extension of the generalized Maxwell model given in eq. (3-2), where $\dot{\gamma}_{ij}$ is replaced by the finite rate-of-strain tensor $\dot{e}^{ij}$ (35)(40)(43) and $\frac{\partial}{\partial t}$ is substituted by the nonlinear operator $\mathcal{J}_{abc}$*. Therefore the Spriggs model can be written as

$$(1 + \lambda_{1p}\mathcal{J}_{abc})\tau_p^{ij} = -\eta_p(1+\lambda_{2p}\mathcal{J}_{abc})\dot{e}^{ij} \qquad (5\text{-}1)$$

where the nonlinear operator is defined by

$$\mathcal{J}_{abc}A^{ij} = \frac{DA^{ij}}{Dt} - \frac{a}{2}(\dot{e}^{ik}A_k^{\ j} + A_k^{\ i}\dot{e}^{kj}) + \frac{b}{2}A_{lmn}\dot{e}^{mn}g^{ij} + \frac{c}{2}A_{mn}g^{mn}\dot{e}^{ij} \qquad (5\text{-}2)$$

In eq. (5-2) $\frac{D}{Dt}$ is the Jaumann derivative.

The inclusion of the rate-of-strain invariant L_2 in the memory function given in eq. (3-5) is an example of the nonlinear integral extension of the generalized Maxwell model where L_2 is defined as

---

* $(\partial\hat{g}^{ij}(\xi,t)\dot{e}^{ij}/\partial t)_\xi$ in the convected coordinate system is defined as where $\hat{g}^{ij}(\xi,t)$ is the convected contravariant metric tensor.

$$\hat{g}_{ij}\,\hat{g}_{rs}\,\frac{d\hat{g}^{ir}}{dt}\,\frac{d\hat{g}^{js}}{dt}$$

so that the memory function in eq. (3-5) can be written as

$$m = m(t-t', I_2)$$

(5.2) Description of Lodge's Network Theory (29)

It is assumed that the polymer solution in the network theory consists of an assembly of very long chain molecules linked together to form a network of segments of various lengths. A given molecule may be linked to the network at two or more points (junctions), but the segment between successive linkages can contain many links (repeating units); the number of repeating units of a segment effectively linked to the network will be different for different segments. The following main assumptions have been made in Lodge's network theory:

(a) The flowing polymer is treated as an imcompressible fluid.

(b) The contribution of the free energy to the stress from the solvent and unattached polymer molecules of segments with loose ends is negligible. The stress is made up of the sum of contributions from all previous time t'. The

contribution to the stress in the interval t' and t'+dt' arises from chain molecules which joined the network and are still part of the network at the current time t; from the kinetic theory of rubber elasticity (45), the concentration of network junctions which were formed in the interval t', t'+dt' and which still exist at the present time t is

$$N(t-t')dt' \qquad (5\text{-}3)$$

where N(t-t') is the network junction age distribution.

(c) The Gaussian network is assumed. The chain molecules are formed from freely-jointed rigid straight links each of length l; when the ends of any chain segment in the network occupy fixed positions of separation r, the number of density of configurations (of equal energy) available to that segment is a Gaussian function

$$P(r) = K \exp\left(\frac{-3r^2}{2nl^2}\right) \qquad (5\text{-}4)$$

where n is the number of links in the segment, and K is a constant whose value is immaterial.

(d) The volume is constant for a constant temperature. From the above assumptions, the following equations are obtained:

$$\tau^{ij} = + \int_{t'=-\infty}^{t} ckT\,N(t-t')\,\hat{g}^{ij}(t')\,dt' \qquad (5\text{-}5\text{-}A)$$

$$= \int_{t'=-\infty}^{t} m(t-t')\,\hat{g}^{ij}(t')\,dt' \qquad (5\text{-}5\text{-}B)$$

$$m(t-t') = ckTN(t-t') \qquad (5\text{-}5\text{-}C)$$

where $m(t-t')$ is a memory function

k is Boltzmann's constant

c is a constant for which the value depends on the structure

T is an absolute temperature

$\hat{g}^{ij}(t')$ is the convected contravariant metric tensor

$N(t-t')$ is the junction age distribution function

τ^{ij} is the convected contravariant stress tensor

(5.3) Memory Functions in the WJFLMB Model and in the Bird-Carreau Model

As pointed out by many previous workers on rheological model building (6)(29)(42), the memory function m(t-t'), which is a function of t-t' only, can be generalized to include the rate-of-strain invariants so that better predictions of the normal-stress differences and the non-Newtonian

viscosities vs. the rates of deformation for polymer solutions are available. Lodge (29) suggests that the memory function m(t-t') can be generalized by allowing the memory function to depend on the second rate-of-strain invariant L_2, which in convected coordinates is defined as*

$$L_2(t') = \hat{g}_{ij}\,\hat{g}_{rs}\,\frac{d\hat{g}^{ir}}{dt'}\,\frac{d\hat{g}^{js}}{dt'} \qquad (5\text{-}6)$$

so that the memory function can be written as

$$m = m(t-t', L_2) \qquad (5\text{-}7)$$

The above modifications of the memory function gives a polymer solution whose non-Newtonian viscosities and normal-stress coefficients θ, β, ε in eqs. (4-3), (4-4) and (4-5) depend on the shear rates at steady-state shearing flow.

The memory function of the WJFLMB model is obtained from Lodge's suggestion that

$$m(t-t', L_2) = m'(t-t')\,m(L_2) \qquad (5\text{-}8)$$

Therefore the shear-rate-dependent memory function is

$$m(t-t', L_2) = \frac{\eta_0}{\sum_{n=1}^{\infty}\lambda_n}\sum_{n=1}^{\infty}\frac{1}{\lambda_n}\,\frac{1}{1+\frac{L_2}{2}c^2\lambda_n^2}\,e^{-\frac{(t-t')}{\lambda_n}} \qquad (5\text{-}9)$$

---

* The summation has been omitted on the right hand side of eq.(5-6).

with $$\lambda_n = \frac{\lambda}{n^{\alpha}}$$

where η_0 is the zero-shear-rate viscosity

λ is a time constant

c is a constant (When c=1, the Weissenberg hypothesis is valid.)

α is a dimensionless parameter

Bird and Carreau (6) extended the WJFLMB model and proposed the memory function as

$$m(t-t', L_2) = \sum_{p=1}^{\infty} \frac{\eta_p}{\lambda_{2p}^2} \frac{1}{1+\frac{L_2}{2}\lambda_{1p}^2} e^{\frac{-(t-t')}{\lambda_{2p}}} \qquad (5\text{-}11)$$

with

$$\eta_p = \eta_0 \frac{\lambda_{1p}}{\sum_{p=1}^{\infty} \lambda_{1p}} \qquad (5\text{-}12\text{-}A)$$

$$\lambda_{1p} = \lambda_1 \left(\frac{1+n_1}{p+n_1}\right)^{\alpha_1} \qquad (5\text{-}12\text{-}B)$$

$$\lambda_{2p} = \lambda_2 \left(\frac{1+n_2}{p+n_2}\right)^{\alpha_2} \qquad (5\text{-}12\text{-}C)$$

where λ_1, λ_2 are two time constants

α_1, α_2 are two dimensionless parameters

n_1, n_2 are two atbitrary constants

In eqs. (5-12-B) and (5-12-C) λ_{1p} and λ_{2p} are two sets of time constants. The use of λ_{1p} and λ_{2p} can be explained by Lodge's network theories; the set of time constants λ_{1p} is associated with the rate of creation of network junctions and λ_{2p} associated with the rate of loss of

network junctions. At the present time the Bird-Carreau model has been recognized as satisfactory in predicting the non-Newtonian viscosities and the primary normal-stress behavior for polymer solutions at both low and intermediate shear rates. However, it is inadequate to predict the rheological properties at high shear rates.*

Development of the Huang-Shangkuan Model

(5.4) A Proposed Memory Function in the Huang-Shangkuan Model

Due to the incapability to predict the rheological properties at high shear rates using the Bird-Carreau model, we generalize the memory function in eq. (5-8) as

$$m(t-t', L_2) = m'(t-t', L_2)\, m''(L_2) \qquad (5\text{-}13)$$

By the use of the above equation, the following memory function can be set up

$$m(t-t', L_2) = \sum_{p=1}^{\infty} \frac{\eta_p(L_2)}{\lambda_{2p}^2(L_2)} \frac{1}{1+\frac{L_2}{2}\lambda_{1p}^2}\, e^{\frac{-(t-t')}{\lambda_{2p}(L_2)}} \qquad (5\text{-}14)$$

in which we postulate the time constant λ_{2p} and the viscosity parameter η_p are dependent on the second rate-of-strain in-

---

* See Figs. 6-5 and 6-6.

variant L_2. This idea is original in comparison with any other previous models.

(5.5) Reduction of Parameters

A rheological equation is of limited value until the parameters are properly reduced. Ideally one would hope to construct a model starting completely from a theory with basic microscopic variables such as chain geometry, molecular weight, etc. However, this approach is not quite successful for polymer solutions at intermediate and high concentrations. For very dilute solutions, there has been good progress, developing from the early theories of Rouse and Buche (19)(39), which apply to linear deformations or to steady-state shearing deformations of high polymers at low shear rates. In other words, these theories are not sufficient to predict shear-dependent viscosities and normal stress differences of concentrated polymer solutions at high shear rates. Proper extensions of Rouse's theory to concentrated polymer solutions result in a very useful rheological model; the unlimited number of parameters in the Huang-Shangkuan model are properly reduced based on the modification of Rouse's theory.

The dilute solution theory of Rouse (39) indicates that

$$\eta_p = \eta_0 \frac{\lambda_p}{\sum_{p=1}^{\infty} \lambda_p} \qquad (5\text{-}15)$$

$$\lambda_p = \frac{\lambda}{p^2} \qquad (5\text{-}16)$$

where η_0 is a zero-shear-rate viscosity

λ is the longest relaxation time which is related to polymer properties such as temperature, degree of polymerization, root-mean-square end-to-end distance of a polymer segment.

Corresponding to eqs. (5-15),(5-16) we consider the following empirisms for the constants in our memory function.

$$\eta_p = \eta_{1p}(\eta_0, \lambda_{1p}) \times \eta_s(L_2)$$

$$= \eta_0 \frac{\lambda_{1p}}{\sum_{p=1}^{\infty} \lambda_{1p}} \times \eta_s(L_2) \qquad (5\text{-}17\text{-}A)$$

$$\lambda_{1p} = \lambda_1 \times \left(\frac{2}{p+1}\right)^{\alpha_1} \qquad (5\text{-}17\text{-}B)$$

$$\lambda_{2p} = \lambda_{2p}(\lambda_2, \alpha_2) \times \lambda_s(L_2)$$

$$= \lambda_2 \left(\frac{2}{p+1}\right)^{\alpha_2} \times \lambda_s(L_2) \qquad (5\text{-}17\text{-}C)$$

where $\eta_s(L_2)$, $\lambda_s(L_2)$ are functions of the second rate-of-strain invariant. Eqs.(5-17-A), (5-17-B), (5-17-C) could be reduced to η_p , λ_{1p} , λ_{2p} in eqs. (5-12-A) to (5-12-C) in the Bird-Carreau model provided that

$$\eta_s(L_2) = \lambda_s(L_2) = 1 \quad ; \quad \eta_1 = \eta_2 = 1$$

(5.6) Choice of Finite Strain Tensors

As shown in chapter 3, the generalized Maxwell equation cannot predict shear-rate-dependent non-Newtonian viscosities and normal stress effects at large rates of deformation; therefore, the replacement of $\gamma_{ij}(t)$ by a finite strain tensor is necessary. There are many finite strain tensors to choose from*, but we select a simple strain tensor (the Finger tensor) which is suggested by continuum mechanics (29). Therefore we replace

$$\gamma_{ij}(t) \qquad \text{by} \qquad \underline{\delta} - \underline{C}^{-1}(t, t_0) \qquad (5\text{-}18)$$

where $\underline{\delta}$ is the Kronecker delta and $\underline{C}^{-1}(t,t_0)$ is the Finger tensor.

(5.7) Expressions of the Finite Strain Tensor and the Second Rate-of-Strain Invariant L_2 at steady State Shearing Flow between Two Parallel Plates

For computational purposes, it is often very handy to have the Finger tensor expressed by Cartesian coordinates. If we denote the Cartesian vector by $\underline{e}_i$, the convected covariant base vector $\underline{g}_\alpha(\xi,t)$ and the convected contravariant base vector $\underline{g}^\alpha(\chi_0)$

---

* In chapter 2, the Cauchy tensor, the Finger tensor, the Green tensor or the Piola tensor with their combinations are the choice for finite strain tensors.

can be expressed in Cartesian coordinates through coordinate transformation

$$\underline{\hat{g}}_\alpha(\xi,t) = \frac{\partial x^i}{\partial \xi^\alpha}\,\underline{g}_i = \frac{\partial x^i}{\partial \xi^\alpha}\,\underline{e}_i \qquad (2\text{-}10)$$

$$\underline{g}^\alpha(X_0) = \underline{e}^\alpha = \underline{e}_\alpha = \underline{g}_\alpha(X_0) \qquad (2\text{-}11)$$

Therefore, the displacement tensor $\underline{\underline{F}}$ and its transpose $\underline{\underline{F}}^T$ in eqs. (2-12-A), and (2-18) in Cartesian coordinates become

$$\underline{\underline{F}} = \underline{\hat{g}}_\alpha(\xi,t)\,\underline{g}^\alpha(X_0) \qquad (2\text{-}13)$$

$$= \left(\frac{\partial x^i}{\partial \xi^\alpha}\right)_t \underline{e}_i\,\underline{e}_\alpha \qquad (5\text{-}19)$$

$$\underline{\underline{F}} = \underline{g}^i(X_0)\,\underline{\hat{g}}_i(\xi,t) \qquad (2\text{-}18)$$

$$= \left(\frac{\partial x^i}{\partial \xi^\alpha}\right)_t \underline{e}_\alpha\,\underline{e}_i \qquad (5\text{-}20)$$

Consider the steady state shearing flow between two parallel plates, which is shown in Fig. 1-1

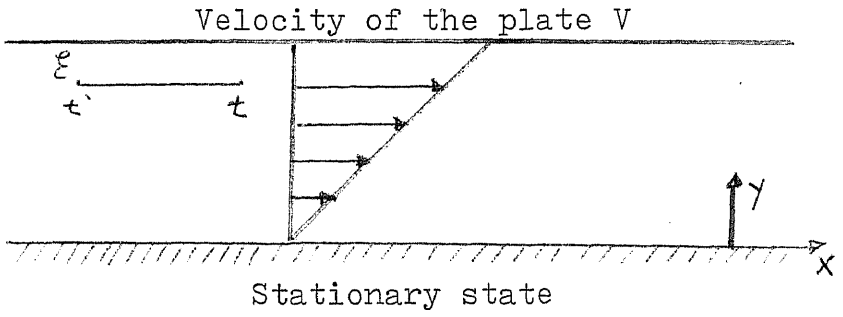

Fig. 1-1 Shear Deformation

where X_i and X_i' are the Cartesian coordinates of a particle ε at time t (present time) and t' (past time) respectively. The velocity profile is

$$v_x = \dot{\gamma} y \quad ; \quad v_y = 0 \quad ; \quad v_z = 0 \tag{5-21}$$

where

$$\dot{\gamma} = \left| \frac{dv_x}{dy} \right|$$

In order to determine $\underline{\underline{F}}$ and $\underline{\underline{F}}^T$, we first integrate eq. (5-21)

$$x' = x - \dot{\gamma} y (t - t') \quad ; \quad y' = y \quad ; \quad z' = z \tag{5-22}$$

Therefore

$$\begin{pmatrix} \frac{\partial x}{\partial x'} & \frac{\partial x}{\partial y'} & \frac{\partial x}{\partial z'} \\ \frac{\partial y}{\partial x'} & \frac{\partial y}{\partial y'} & \frac{\partial y}{\partial z'} \\ \frac{\partial z}{\partial x'} & \frac{\partial z}{\partial y'} & \frac{\partial z}{\partial z'} \end{pmatrix} = \begin{pmatrix} 1 & \dot{\gamma}(t-t') & 0 \\ 0 & 1 & 0 \\ 0 & 0 & 1 \end{pmatrix} \tag{5-23}$$

Take the particle $\mathcal{E}$ at time t' as the reference state t_0; therefore $\mathcal{E}^{t'} = (x', y', z')$ and $x^{t'} = (x, y, z)$. From eqs. (5-19) and (5-20)

$$\underline{\underline{F}} = \begin{pmatrix} \frac{\partial x}{\partial x'} & \frac{\partial x}{\partial y'} & \frac{\partial x}{\partial z'} \\ \frac{\partial y}{\partial x'} & \frac{\partial y}{\partial y'} & \frac{\partial y}{\partial z'} \\ \frac{\partial z}{\partial x'} & \frac{\partial z}{\partial y'} & \frac{\partial z}{\partial z'} \end{pmatrix} = \begin{pmatrix} 1 & \dot{\gamma}(t-t') & 0 \\ 0 & 1 & 0 \\ 0 & 0 & 1 \end{pmatrix} \tag{5-24}$$

$$\underline{\underline{F}}^T = \begin{pmatrix} 1 & 0 & 0 \\ \dot{\gamma}(t-t') & 1 & 0 \\ 0 & 0 & 1 \end{pmatrix} \tag{5-25}$$

The Finger tensor, which is defined in eq. (2-21), is equal to

$$\underline{\underline{C}}^{-1}(t,t_0) = \underline{\underline{C}}^{-1}(t,t') = \underline{\underline{F}} \cdot \underline{\underline{F}}^T$$

$$= \begin{pmatrix} 1 & \dot{\gamma}(t-t') & 0 \\ 0 & 1 & 0 \\ 0 & 0 & 1 \end{pmatrix} \begin{pmatrix} 1 & 0 & 0 \\ \dot{\gamma}(t-t') & 1 & 0 \\ 0 & 0 & 1 \end{pmatrix}$$

$$= \begin{pmatrix} 1+\dot{\gamma}^2(t-t')^2 & \dot{\gamma}(t-t') & 0 \\ \dot{\gamma}(t-t') & 1 & 0 \\ 0 & 0 & 1 \end{pmatrix} \qquad (5\text{-}26)$$

Therefore the finite strain tensor in eq. (5-18) becomes

$$\underline{\underline{\delta}} - \underline{\underline{C}}^{-1}(t,t_0) = \underline{\underline{\delta}} - \underline{\underline{C}}^{-1}(t,t') = \begin{pmatrix} -\dot{\gamma}^2(t-t')^2 & -\dot{\gamma}(t-t') & 0 \\ -\dot{\gamma}(t-t') & 0 & 0 \\ 0 & 0 & 0 \end{pmatrix} \qquad (5\text{-}27)$$

From eq. (5-6), L_2 in convected coordinates is defined as

$$L_2 = \hat{g}_{ij}\,\hat{g}_{rs}\,\frac{d\hat{g}^{ir}}{dt}\,\frac{d\hat{g}^{js}}{dt} \qquad (5\text{-}6)$$

which could be written in fixed coordinates as

$$L_2 = g_{ij}(x)\,g_{rs}(x)\,\dot{e}^{ir}\,\dot{e}^{js} \qquad (5\text{-}28)$$

where $\dot{e}^{ir}$ or $\dot{e}^{js}$ are the components of the rate-of-strain tensor given in section (4-1).

In the Cartesian coordinate system, L_2 in eq. (5-28)

can be further simplified to

$$L_2 = \delta_{ij}\delta_{rs}\dot{\gamma}^{ir}\dot{\gamma}^{js} = \dot{\gamma}^{ir}\dot{\gamma}^{ir} \qquad (5\text{-}29)$$

At steady state shearing flow, the shear rate is

$$\dot{\gamma}^{ir} = \begin{pmatrix} 0 & \dot{\gamma}^{12} & 0 \\ \dot{\gamma}^{12} & 0 & 0 \\ 0 & 0 & 0 \end{pmatrix} \qquad (5\text{-}30)$$

Therefore

$$L_2 = 2(\dot{\gamma}^{12})^2 = 2\dot{\gamma}^2 \qquad (5\text{-}31)$$

where

$$\dot{\gamma} = |\dot{\gamma}^{xy}| = |\dot{\gamma}^{12}| = \left|\frac{dv_x}{dy}\right|$$

From eq. (5-31), it is understood that L_2 is closely related to the shear rate. This is very helpful to correlate shear-rate-dependent material functions to the invariant property (L_2).

(5.8) Expressions of Shear Stress and Normal Stress Difference at Steady-State Shearing Flow between Two Parallel Plates

After eqs. (5-14) and (5-27) are combined, the pro-

posed rheological model can be written in the matrix from as*

$$\underline{\underline{\mathcal{J}}} = -\int_{-\infty}^{t} m_1(t-t', L_2) \times \left[\underline{\underline{C}}^{-1}(t,t') - \underline{\underline{\delta}}\right] dt' \qquad (5\text{-}32)$$

$$\begin{pmatrix} \mathcal{J}^{11} & \mathcal{J}^{12} & \mathcal{J}^{13} \\ \mathcal{J}^{21} & \mathcal{J}^{22} & \mathcal{J}^{23} \\ \mathcal{J}^{31} & \mathcal{J}^{32} & \mathcal{J}^{33} \end{pmatrix} = \int_{-\infty}^{t} \left\{ \sum_{p=1}^{\infty} \frac{\eta_p(L_2)}{\lambda_{2p}^2(L_2)} \frac{1}{1+\frac{L_2}{2}\lambda_{1p}^2} e^{\frac{-(t-t')}{\lambda_{2p}(L_2)}} \right\}$$

$$\times \begin{pmatrix} -\dot{\gamma}^2(t-t')^2 & -\dot{\gamma}(t-t') & 0 \\ -\dot{\gamma}(t-t') & 0 & 0 \\ 0 & 0 & 0 \end{pmatrix} dt' \qquad (5\text{-}33)$$

From the above equation, the following components are obtained:

$$-\mathcal{J}^{12} = \sum_{p=1}^{\infty} \frac{\eta_p(L_2)}{\lambda_{2p}^2(L_2)} \frac{1}{1+\frac{L_2}{2}\lambda_{1p}^2} \int_{-\infty}^{t} e^{\frac{-(t-t')}{\lambda_{2p}(L_2)}} \dot{\gamma}(t-t')\, dt' \qquad (5\text{-}34)$$

---

* At steady-state shearing flow the notation (x,y,z) = (1,2,3)

$$-(\mathcal{J}^{11}-\mathcal{J}^{22}) = \sum_{p=1}^{\infty} \frac{\eta_p(L_2)}{\lambda_{2p}^2(L_2)} \frac{1}{1+\frac{L_2}{2}\lambda_{1p}^2} \int_{-\infty}^{t} e^{\frac{-(t-t')}{\lambda_{2p}(L_2)}} \dot{\gamma}^2(t-t')^2 dt' \quad (5\text{-}35)$$

$$-(\mathcal{J}^{22}-\mathcal{J}^{33}) = 0 \quad (5\text{-}36)$$

The integrals in eqs. (5-34), (5-35) are easy to compute by use of

$$\int_{-\infty}^{t} e^{\frac{-(t-t')}{\lambda_{2p}(L_2)}} (t-t')^n dt' = n!\, \lambda_{2p}^{n+1} \quad (5\text{-}37)$$

and we get

$$-\mathcal{J}^{12} = \sum_{p=1}^{\infty} \frac{\eta_p(L_2)}{1+\frac{L_2}{2}\lambda_{1p}^2} \dot{\gamma} \quad (5\text{-}38)$$

$$-(\mathcal{J}^{11}-\mathcal{J}^{22}) = 2\sum_{p=1}^{\infty} \frac{\eta_p(L_2) \times \lambda_{2p}(L_2)}{1+\frac{L_2}{2}\lambda_{1p}^2} \quad (5\text{-}39)$$

Therefore

$$\eta = \sum_{p=1}^{\infty} \frac{\eta_p(L_2)}{1+\frac{L_2}{2}\lambda_{1p}^2}$$

and

$$\theta = 2 \sum_{p=1}^{\infty} \frac{\eta_p(L_2) \times \lambda_{2p}(L_2)}{1 + \frac{L_2}{2} \lambda_{1p}^2} \qquad (5\text{-}41)$$

Some interesting results can be observed from η and θ in the above two equations: θ contains η_p , λ_{1p} , λ_{2p} but η contains only η_p and λ_{1p} . In the limit case that $\lambda_{2p} = 0$, the model could describe purely viscous fluids without normal-stress effect.

(5-9) Asymptotic Expressions for the Material Functions at High Shear Rate

The material functions in eqs. (5-40) and (5-41) are not very useful until the unlimited sets of constants $\eta_p(L_2)$, $\lambda_{2p}(L_2)$ and η_{1p} are reduced. It has been shown that $L_2 = 2\dot{\gamma}^2$ in eq. (5-31) at steady-state shearing flow. After substituting L_2, $\eta_p(L_2)$, λ_{1p} , $\lambda_{2p}(L_2)$ given in section (5-5) into eqs. (5-40) and (5-41) and rearranging them, we obtain

$$\frac{\eta}{\eta_0} = \underbrace{\left\{ 1 - \frac{(2^{\alpha_1}\lambda_1\dot{\gamma})^2}{2(\alpha_1)-1} \sum_{p=1}^{\infty} \frac{p^{-\alpha_1}}{p^{2\alpha_1} + (2^{\alpha_1}\lambda_1\dot{\gamma})^2} \right\}}_{(A)} \times \eta_s(2\dot{\gamma}^2) \qquad (5\text{-}42)$$

and

$$\frac{\theta}{\eta_0} = \left\{ \frac{2^{\alpha_2+1}\lambda_2}{\zeta(\alpha_1)-1} \left[\zeta(\alpha_1+\alpha_2) - 1 - (2^{\alpha_1}\lambda_1\dot{\gamma})^2 \times \sum_{p=2}^{\infty} \frac{p^{-(\alpha_1+\alpha_2)}}{p^{2\alpha_1}+(2^{\alpha_1}\lambda_1\dot{\gamma})^2} \right] \right\} \qquad (C)$$

$$\times \eta_s(2\dot{\gamma}^2) \times \lambda_s(2\dot{\gamma}^2) \qquad (5\text{-}43)$$

where $\zeta(\alpha) = \sum_{p=1}^{\infty} p^{-\alpha}$ is the Riemann-Zeta function. Only the first few terms of the above rapidly convergent series are necessary to determine η and θ at low shear rates. However, for large shear rates, the asymptotic expression in a closed form are obtained by use of the Euler-Maclaurin sum formula (37) (12)*:

$$\frac{\eta}{\eta_0} \to \frac{1}{\zeta(\alpha_1)-1} \left[\frac{\Pi (2^{\alpha_1}\lambda_1\dot{\gamma})^{\frac{1-\alpha_1}{\alpha_1}}}{2\alpha_1 \sin\left(\frac{(1+\alpha_1)\pi}{2\alpha_1}\right)} \right] \times \eta_s(2\dot{\gamma}^2) \qquad (5\text{-}44)$$

$$\frac{\theta}{\eta_0} \to \frac{2^{\alpha_2+1}\lambda_2}{\zeta(\alpha_1)-1} \left[\frac{\Pi (2^{\alpha_1}\lambda_1\dot{\gamma})^{\frac{1-\alpha_1-\alpha_2}{\alpha_1}}}{2\alpha_1 \sin\left(\frac{(1+\alpha_1-\alpha_2)\pi}{2\alpha_1}\right)} \right] \times \eta_s(2\dot{\gamma}^2) \times \lambda_s(2\dot{\gamma}^2) \qquad (5\text{-}45)$$

In consideration of $\eta_s(2\dot{\gamma}^2)$ and $\lambda_s(2\dot{\gamma}^2)$ in the above two

---

* The detailed derivations of the asymptotic expressions of part (A) and part (C) in eqs. (5-42) and (5-43) at high shear rates refer to reference (12).

equations, there could be many choices. But we select one simple form:

$$\eta_s(2\dot{\gamma}^2) = e^{a\dot{\gamma}^b} \tag{5-46}$$

$$\lambda_s(2\dot{\gamma}^2) = e^{c\dot{\gamma}^d} \tag{5-47}$$

where a, b, c and d are dimensionless parameters. Therefore, we can rewrite the material functions as

$$\frac{\eta}{\eta_0} = \underbrace{\frac{1}{2(\alpha_1)-1}\left[\frac{\pi(2^{\alpha_1}\lambda_1\dot{\gamma})^{\frac{1-\alpha_1}{\alpha_1}}}{2\alpha_1 \sin\left(\frac{(1+\alpha_1)\pi}{2\alpha_1}\right)}\right]}_{(A)} \times \underbrace{e^{a\dot{\gamma}^b}}_{(B)} \tag{5-48}$$

$$\frac{\theta}{\eta_0} = \underbrace{\frac{2^{\alpha_2+1}\lambda_2}{2(\alpha_1)-1}\left[\frac{\pi(2^{\alpha_1}\lambda_1\dot{\gamma})^{\frac{1-\alpha_1-\alpha_2}{\alpha_1}}}{2\alpha_1 \sin\left(\frac{(1+\alpha_1-\alpha_2)\pi}{2\alpha_1}\right)}\right]}_{(C)} \times \underbrace{e^{a\dot{\gamma}^b}}_{(B)} \times \underbrace{e^{c\dot{\gamma}^d}}_{(D)} \tag{5-49}$$

In the above two equations, there are a total number of nine parameters:

η_0 is the zero-shear-rate viscosity

λ_1, λ_2 are time constants

α_1, α_2 are dimensionless parameters related to power-law behavior

a, b, c, d are dimensionless parameters related to experimental observations at high shear rates.

(5.10) A Method of Nonlinear Parameter Estimation

Due to the complicated behavior of polymer solutions, the usual nonlinear least-square method fails to predict the parameters in our model. Instead, the method of superposition is applied; the first approximation in estimating the parameters from experimental observations can be made by the analysis of eqs. (5-48) and (5-49) in which, for convenience, we label

$$(A): \quad \frac{1}{\Gamma(\alpha_1)-1}\left[\frac{\pi\left(2^{\alpha_1}\lambda_1\dot{\gamma}\right)^{\frac{1-\alpha_1}{\alpha_1}}}{2\alpha_1 \sin\left(\frac{(1+\alpha_1)\pi}{2\alpha_1}\right)}\right] \qquad (5\text{-}50\text{-}A)$$

$$(A'): \quad (A)\times\dot{\gamma} \qquad (5\text{-}50\text{-}B)$$

$$(B): \quad e^{a\dot{\gamma}^b} \qquad (5\text{-}51)$$

$$(C): \quad \frac{2^{\alpha_2+1}\lambda_2}{\Gamma(\alpha_1)-1}\left[\frac{\pi\left(2^{\alpha_1}\lambda_1\dot{\gamma}\right)^{\frac{1-\alpha_1-\alpha_2}{\alpha_1}}}{2\alpha_1 \sin\left(\frac{(1+\alpha_1-\alpha_2)\pi}{2\alpha_1}\right)}\right] \qquad (5\text{-}52\text{-}A)$$

$$(C'): \quad (C)\times\dot{\gamma}^2 \qquad (5\text{-}52\text{-}B)$$

$$(D): \quad e^{c\dot{\gamma}^d} \qquad (5\text{-}53)$$

Therefore both equations (5-48) and (5-49) are rewritten as

$$\frac{\eta}{\eta_0} = (A)\ (B) \qquad (5\text{-}54\text{-}A)$$

$$\frac{\tau_{12}}{\eta_0} = (A')\ (B) \qquad (5\text{-}54\text{-}B)$$

$$\frac{\theta}{\eta_0} = (C)\ (B)\ (D) \qquad (5\text{-}55\text{-}A)$$

$$\frac{-(\tau_{11}-\tau_{22})}{\eta_0} = (C')\ (B)\ (D) \qquad (5\text{-}55\text{-}B)$$

Generally the experimental data of the non-Newtonian viscosity vs. the shear rate of high polymers can be visualized as four regions shown in Fig. 5-1 where

region I : the viscosity is nearly constant at quite low shear-rate region.

region II : the transition period is between region I and the power-law region (region III).

region III : in this region, the slope of viscosity vs. shear rate is approximately constant (power-law region).

region IV : the slope of log η vs. log $\dot{\gamma}$ deviates from that in the power-law region and increases steadily. For some polymeric fluids of which the region IV does not exist*,

---

* As suggested by Dr. Huang and Dr. Phillipoff, approximately 10% of polymer solutions could have the existence of region IV.

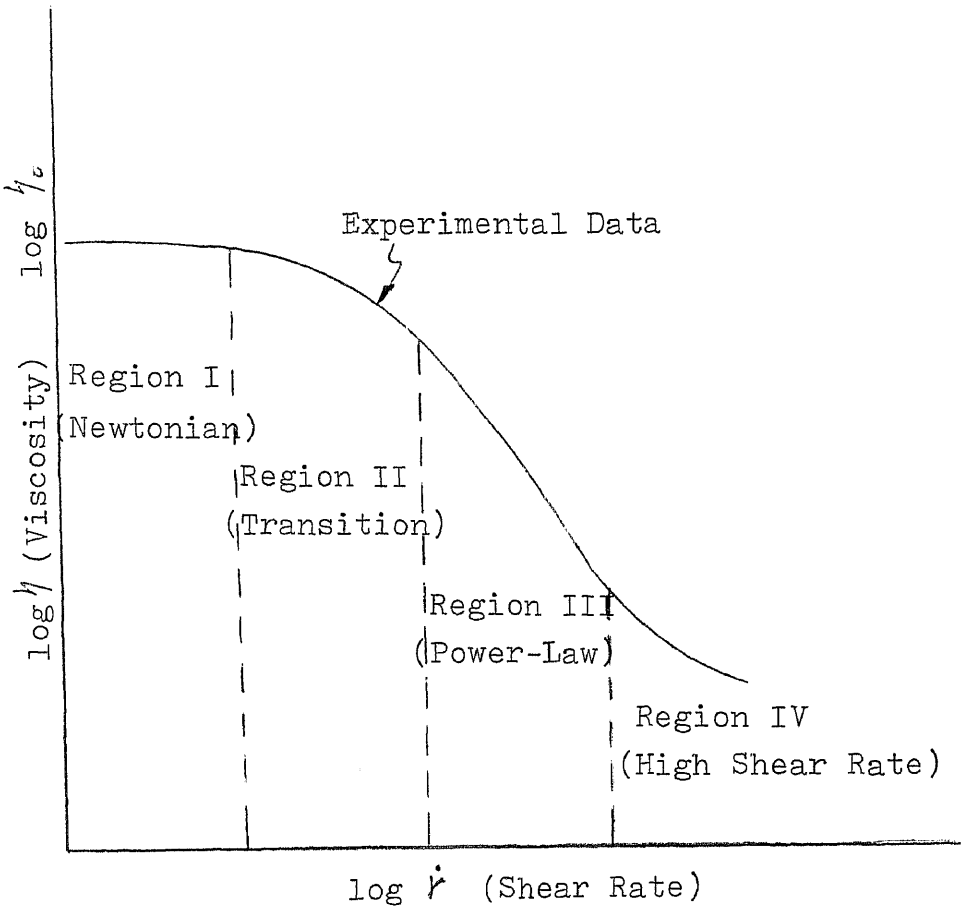

Fig. 5-1 Experimental Non-Newtonian Viscosity vs. Shear Rate for Polymeric Fluids

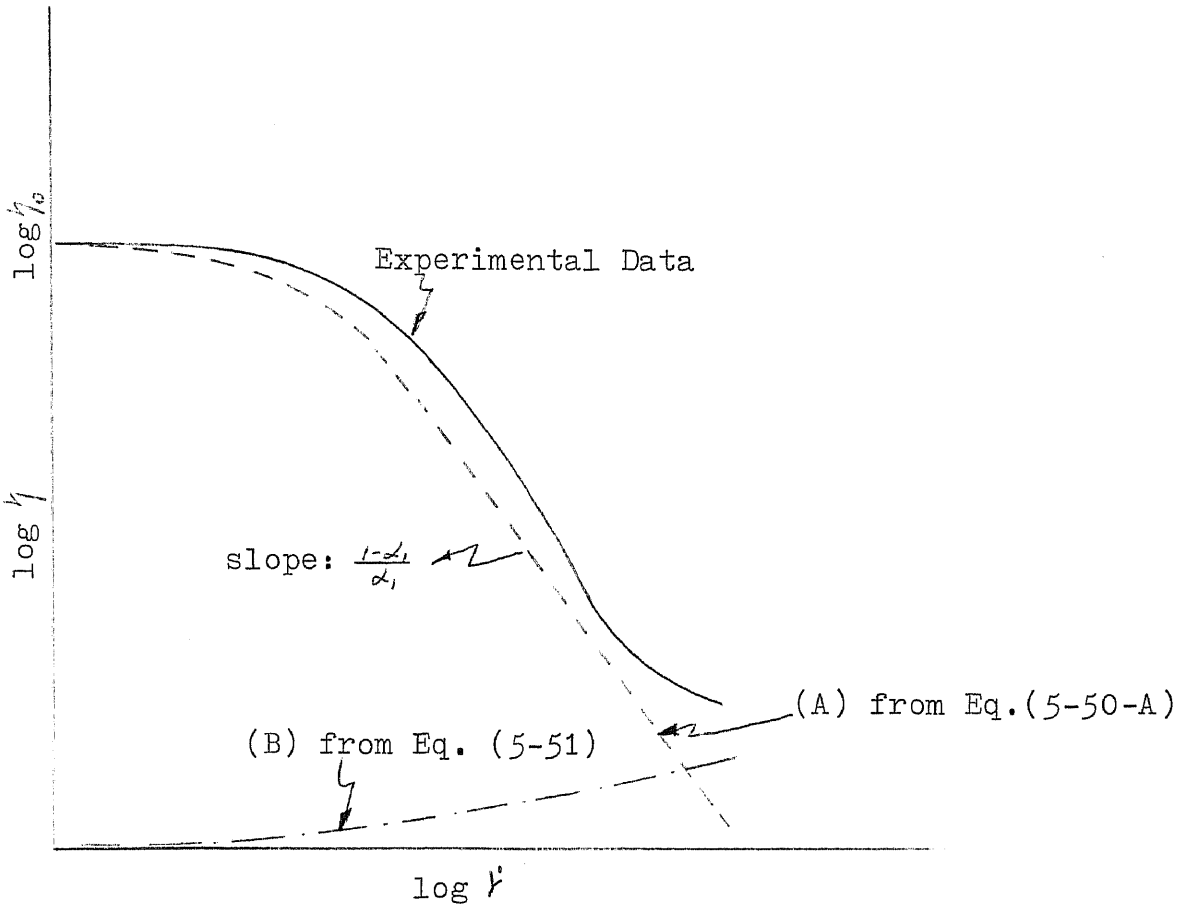

Fig. 5-2 Non-Newtonian Viscosity vs. Shear Rate for Polymeric Fluids

therefore, the power-law region extends directly to region IV.

The procedures to estimate parameters are

(a) When $\dot{\gamma} \to 0$, $\eta \to \eta_0$ where η_0 , the viscosity at zero shear rate, can be estimated from Fig. 5-1 or obtained from the literature.

(b) From eq. (5-50-A) and the slope $(\frac{1-\alpha_1}{\alpha_1})$ of the curve (A) in region III in Fig. 5-2, α_1 and λ_1 are evaluated.

(c) The evaluation of parameters a, b from eq. (5-51) and the curve (B) in Fig. 5-2 are based on the technique of pattern search (49). In the pattern search, an objective function must be applied. We define an objective function as SUM= $\sum_{i=1}^{n} ((Y_i - \hat{Y}_i)/\hat{Y}_i)^2$ where $\hat{Y}_i$ from the curve (B) in Fig. 5-2 is regarded as a set of data points and Y_i is computed from eq. (5-51). When the program of pattern search continues, the optimal values of parameters a and b are computed after the objective function SUM reaches the minimum value (49).

(d) Similar to the procedure in part (b), α_2 and λ_2 in eq. (5-52-A) are obtained from the slope $(\frac{1-\alpha_1-\alpha_2}{\alpha_2})$ of the curve of log C' vs. log $\dot{\gamma}$ shown in Fig. 5-3*.

(e) By use of the same procedure for the non-Newtonian viscosity given in part (c), parameters c and d can be estimated from eq. (5-53) and the curve (D) in Fig. 5-3.

(f) By incorporating the initial values of parameters from

---

* Log θ vs. Log $\dot{\gamma}$ has the similar curve as that of the non-Newtonian viscosity as shown in Fig. 5-1. Note that $-(\tau_{11}-\tau_{22})/\eta_0$ is the superposition of three curves (C'),(B) and (D).

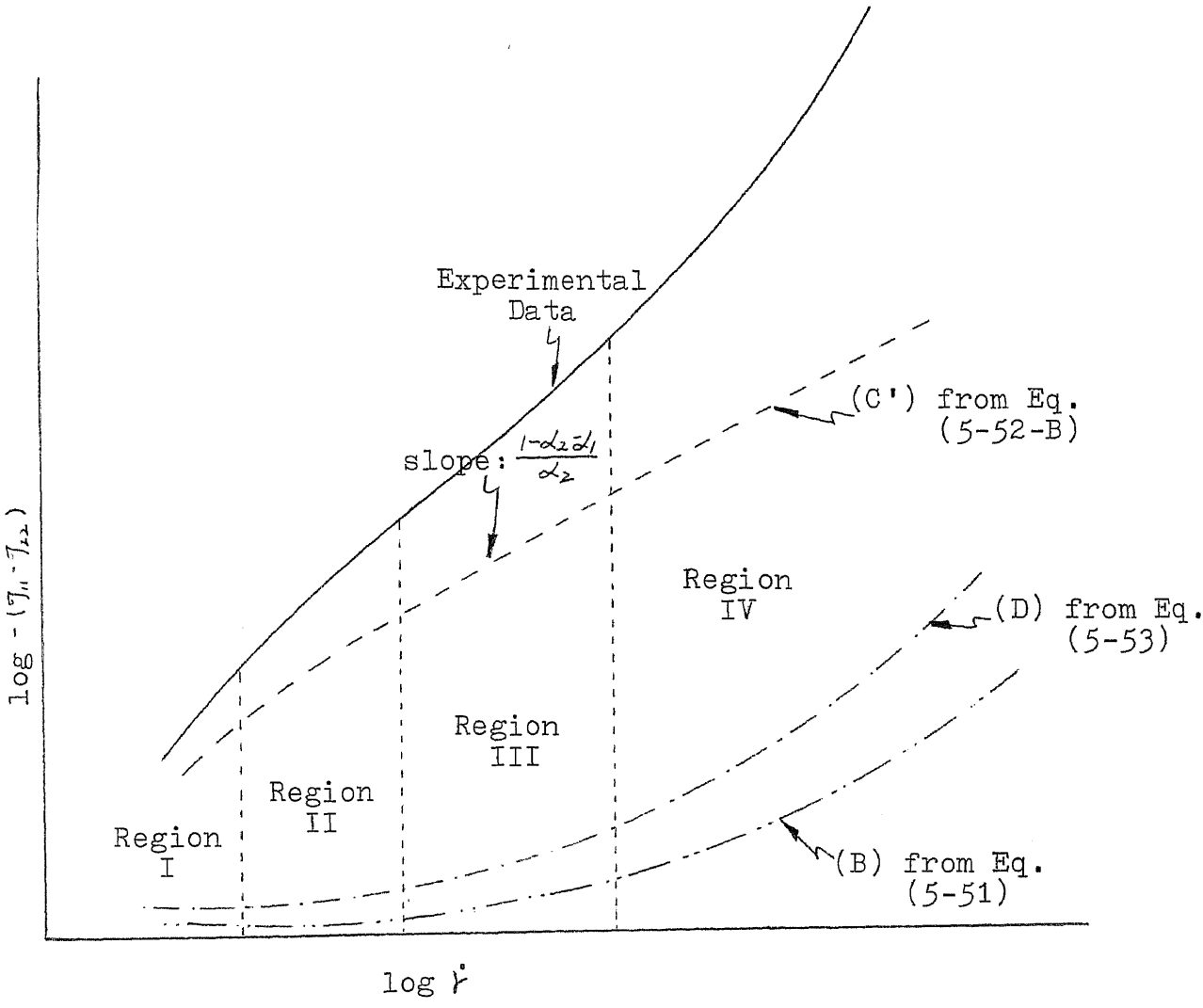

Fig. 5-3 Normal-Stress Differences vs. Shear Rates for Polymeric Fluids

steps (a) to (e) and the experimental data in Figs. 5-2 and 5-3 as the input to the computer program in Appendix 2, a final adjustment of the input parameters can be executed in order to get an optimum set of parameters. The technique used in the computer program is based on the pattern-search technique. The objective function associated with this technique is defined as $\sum_{i=1}^{n}((Y_i-\hat{Y}_i)/\hat{Y}_i)^2$ where $\hat{Y}_i$ is a set of data points of η or $-(\mathcal{T}_{11}-\mathcal{T}_{22})$ and Y_i is computed from eq. (5-54-A) or from eq. (5-55-B).

(5.11) Description of the Spriggs and Bird-Carreau Models

In order to compare our model with the other models in the next chapter, we describe simply the Spriggs model and the Bird-Carreau model here. The Spriggs model is a nonlinear extension of the generalized differential Maxwell model given in eq. (3-2). This model is treated as a special case of the following equation (35)(43).

$$(1+\lambda_{1p}\mathcal{J}_{\mu_1 v_1 \mu_0})\mathcal{T}_p^{ij} = -\eta_p(1+\lambda_{2p}\mathcal{J}_{\mu_2 v_2 \mu_0})\dot{e}^{ij} \qquad (5\text{-}56)$$

where the nonlinear operator is defined by

$$\mathcal{J}_{abc}A^{ij} = \frac{DA}{Dt} - \frac{a}{2}(\dot{e}^{ik}A_k^j + A_k^i\dot{e}^{kj}) + \frac{b}{2}A_{mn}\dot{e}^{mn}g^{ij} + \frac{c}{2}A_{mn}g^{mn}\dot{e}^{ij} \qquad (5\text{-}57)$$

$\frac{\mathcal{D}}{\mathcal{D}t}$ is the Jaumann derivative in the above equation (52).

Spriggs has proposed a 4-constant model by setting $\mu_0 = 0$, $\nu_1 = \frac{2}{3}\mu_1$, $\nu_2 = \frac{2}{3}\mu_2$. The unlimited number of parameters λ_{1p}, and η_p are reduced by modifying Rouse's theory:

$$\lambda_{1p} = \frac{\lambda}{p^\alpha} \tag{5-58}$$

$$\eta_p = \frac{\eta_0}{\mathcal{Z}(\alpha) p^\alpha} \tag{5-59}$$

where λ is a time constant, η_0 is the zero shear viscosity and $\mathcal{Z}(\alpha)$ is the Riemann zeta function. The following material functions are derived from eqs. (5-56) to (5-59) at steady-state shearing flow

$$\frac{\eta}{\eta_0} = \frac{1}{\mathcal{Z}(\alpha)-1} \sum_{p=2}^{\infty} \frac{p^\alpha}{p^{2\alpha} + (C\lambda\dot{\gamma})^2} \tag{5-60}$$

$$\frac{\theta}{\eta_0} = \frac{2^{\alpha+1} \lambda \eta_0}{\mathcal{Z}(\alpha)-1} \sum_{p=2}^{\infty} \frac{1}{p^{2\alpha} + (C\lambda\dot{\gamma})^2} \tag{5-61}$$

where $C = (2/3)^{\frac{1}{2}}$ when the Weissenberg hypothesis is used. There are a total of four constants η_0, α, λ, C in the Spriggs model.

By the use of the memory function in eqs. (5-11) to (5-12-C) and the finite strain tensor in eq. (5-27), Bird and Carreau generalize the Maxwell equation (3-5) given in

integral form. Therefore, the following material functions at steady-state shearing flow are obtained:

$$\frac{\eta}{\eta_0} = \frac{1}{2(\alpha_1)-1} \sum_{p=2}^{\infty} \frac{p^{\alpha_1}}{p^{2\alpha_1}+(2^{\alpha_1}\lambda_1\dot{\gamma})^2} \tag{5-62}$$

$$\frac{\theta}{\eta_0} = \frac{2^{\alpha_1+1}\lambda_2}{2(\alpha_1)-1} \sum_{p=2}^{\infty} \frac{p^{\alpha_1-\alpha_2}}{p^{2\alpha_1}+(2^{\alpha_1}\lambda_1\dot{\gamma})^2} \tag{5-63}$$

where five parameters are included: η_0 , α_1 , α_2 , λ_1 and λ_2 .

CHAPTER 6 EXPERIMENTAL EVALUATION OF THE MODELS

(6.1) Introduction of the Weissenberg Rheogoniometer

The experimental data in this thesis was taken with a Weissenberg Rheogoniometer, a cone and plate apparatus which can be used to measure shear and normal stresses for steady rotation and/or oscillatory motion. The fluid to be tested is placed between the cone and the plate. If the angle between the cone and the plate is small enough, the shear rate in the fluid is very nearly uniform throughout the gap. Measurement of rotational speed and torque required to drive the cone yields the shear rate vs. shear stress relation of the fluid. The amount of normal force that results from this specimen can be found through the measurement of total force exerted by the specimen on the bottom platen. In Fig. 6-1 is a typical arrangement of the Weissenberg Rheogoniometer which was designed by Weissenberg and manufactured by Farol Research Engineers Ltd., England. Due to its precise measurements and simplified working equations to predict rheological properties, the Weissenberg Rheogoniometer is now widely used both commercially and academically. It consists of three major parts; the drive unit, the measuring unit and the control unit with read-out system.

(a) the drive unit: At the left side in Fig. 6-1 is the drive unit which contains a 1 h.p. 1800 RPM synchronous

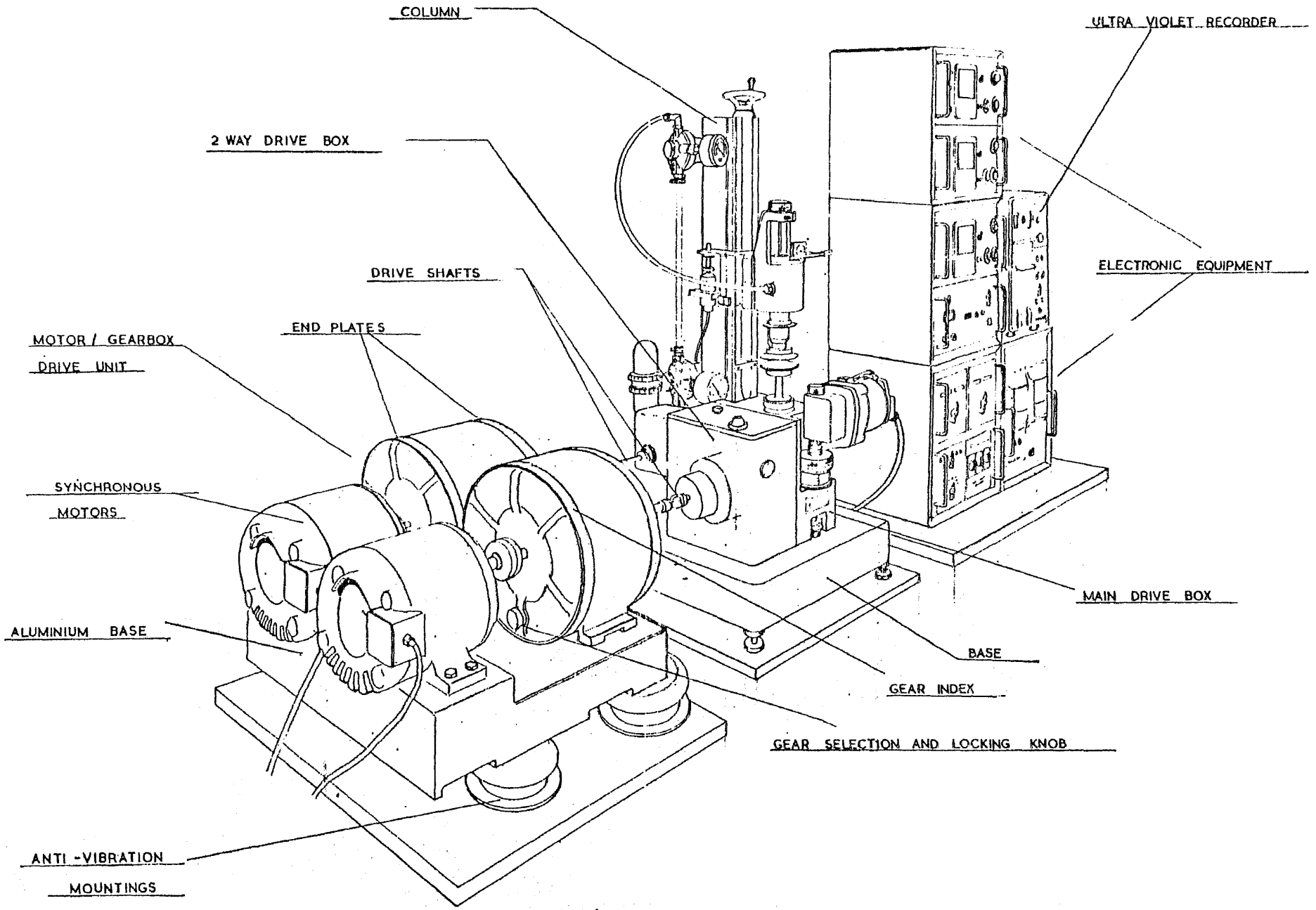

Fig.6-1 TYPICAL ARRANGEMENT OF THE WEISSENBERG RHEOGONIOMETER

motor driving a gear box next to it with gear ratios from 1:1 to $1:10^{-5.9}$ in sixty logarithmic steps. The drive from the gear box is transmitted into the electromagnetic brake/drive at the left-hand side of the measuring unit. The drive passes from the brake unit into a two-way drive box and then into the main drive box. A bronze spur gear on the drive shaft in the two-way drive box transfers the drive to a horizontal 4-start worm via a steel spur gear near the left end of the worm. A horizontal worm gear in the main drive box transfers the drive to the lower platen shaft of the cone-and-plate viscometer.

(b) the measuring unit (central part in Fig. 6-1): It is rigidly constructed and contains the cone-and-plate viscometer (Fig. 6-2).

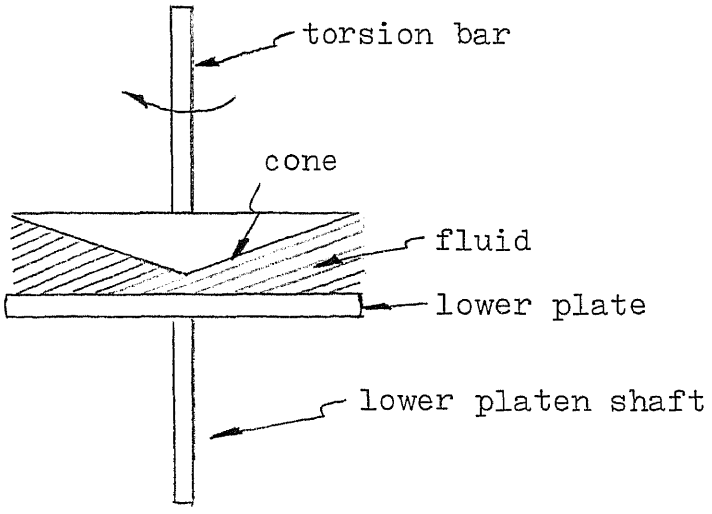

Fig. 6-2 Simplified Picture of the Cone-and-Plate Viscometer in the Measuring Unit of the Weissenberg Rheogoniometer

The torsion bar in Fig. 6-2 is used to detect the movement of the upper cone in order to get the shear stress. The lower platen shaft can take the total force acting on the lower plate by the specimen. The total force can be transmitted to press a leaf spring beneath the lower platen shaft (Fig. 6-3). The rear end of the leaf spring is held rigidly as a cantilever in a rigid block. The leaf spring has its free end on line with the micrometer and the spring loaded plunger vertically. As the normal force is increased, the leaf spring will be deflected. But its deflection can be adjusted to zero through the functions of the servo motor and the spring loaded plunger. In other words the spring loaded plunger will lift the free end of the leaf spring to zero position and the servo motor, at the same time, absorbs the deflection on the leaf spring exerted by the lower platen shaft. Therefore the total force can be obtained by the product of the reading of the micrometer and the spring rate of the leaf spring.

(c) the control unit with read-out system: This part of the instrument (Fig. 6-1) consists of various controllers and recorders. The signals from the transducers are picked up by "Penderford multimeters" whose signals can, in turn, be displayed on an x-y recorder or photographed from an oscilloscope screen. The transducer meter is calibrated to read linear displacement directly in microns with ranges

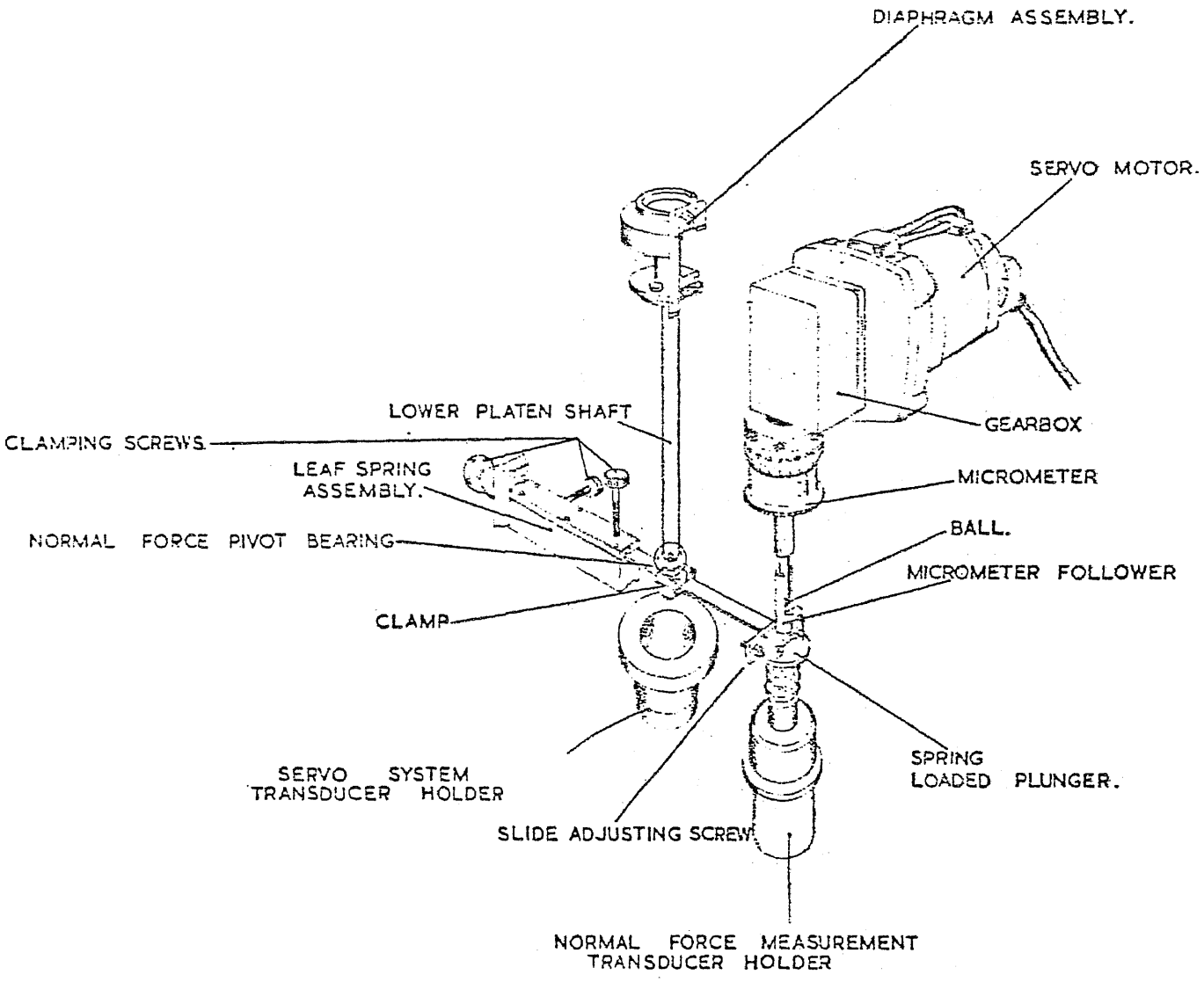

Fig. 6-3 ARRANGEMENT OF NORMAL FORCE MEASUREMENT

from 5 to 2000 microns of full-scale deflection.

(6-2) Working Equations for the Computation of Non-Newtonian Viscosities, Primary Normal-Stress Difference and Shear Rates in a Cone-and-Plate Viscometer

We use a system of spherical polar coordinates $(1, 2, 3)=(\phi, \theta, r)$ in which the origin is C and the axis $\theta = 0$ is vertically upwards. Let the angular velocity of the lower platen shaft be Ω_0. We consider a state of flow for a fluid filling the gap between plate and cone is such

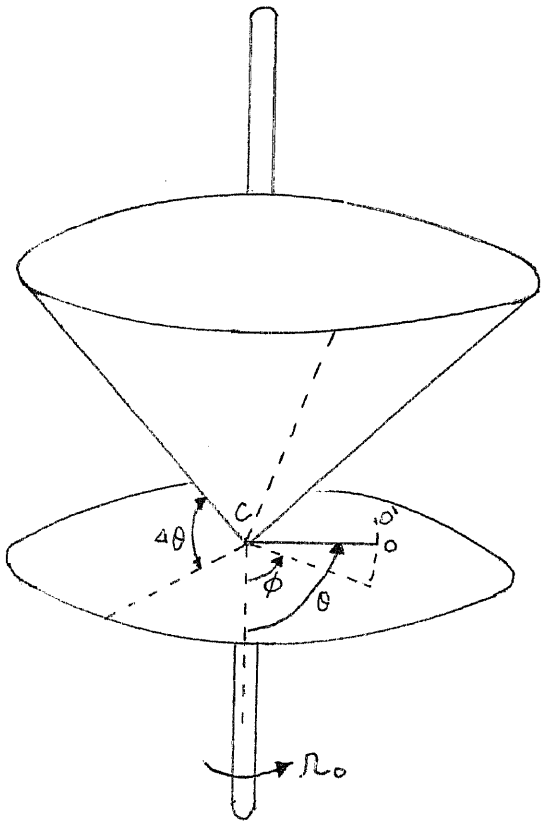

Fig. 6-4 Spherical Polar Coordinates System (Origin C) for Shear Flow between a Cone-and-Plate in Relative Rotation

that the angular velocity Ω of the liquid varies from the value Ω_0 at the plate to the value zero at the cone $\theta=\frac{\pi}{2}+\Delta\theta$; therefore, $\Omega=\Omega(\theta)$.

(a) working equations of shear stresses and non-Newtonian viscosities

The equations of motion in a spherical polar coordinate system can be applied to derive these working formulas. The ϕ-component of the equation of motion is

$$\rho\left(\frac{\partial v_\phi}{\partial t}+v_r\frac{\partial v_\phi}{\partial r}+\frac{v_\theta}{r}\frac{\partial v_\phi}{\partial\theta}+\frac{v_\phi}{r\sin\theta}\frac{\partial v_\phi}{\partial\phi}+\frac{v_\phi v_r}{r}+\frac{v_\theta v_\phi}{r}\cot\theta\right)$$

$$=-\frac{1}{r\sin\theta}\frac{\partial p}{\partial\phi}-\left[\frac{1}{r^2}\frac{\partial}{\partial r}(r^2\tau_{r\phi})+\frac{1}{r}\frac{\partial\tau_{\theta\phi}}{\partial\theta}+\frac{1}{r\sin\theta}\frac{\partial\tau_{\theta\phi}}{\partial\phi}\right.$$

$$\left.+\frac{\tau_{r\phi}}{r}+\frac{2\cot\theta}{r}\tau_{\theta\phi}\right]+\rho g_\phi \qquad (6\text{-}1)$$

Assume that the fluid in the gap of cone-and-plate is under steady-state shearing flow. Therefore the following assumptions are valid (8).

$$\tau_{r\phi}=\tau_{r\theta}=\tau_{\phi r}=\tau_{\theta r}=0 \qquad (6\text{-}2\text{-A})$$

$$v_\phi=rf(\theta)\ ;\ v_\theta=0\ ;\ v_r=0 \qquad (6\text{-}2\text{-B})$$

and

$$\tau_{\phi\phi} - \tau_{\theta\theta}\,,\quad \tau_{\theta\theta} - \tau_{rr}\,,\quad \tau_{\theta\phi} = \tau_{\phi\theta} \qquad (6\text{-}2\text{-}C)$$

depend only on the shear rate $\dot{\gamma}$.

Because of the symmetry of the state of flow with respect to arbitrary rotations about the cone axis. Therefore

$$\frac{\partial \tau_{\phi\theta}}{\partial \phi} = \frac{\partial \tau_{\phi\phi}}{\partial \phi} = \frac{\partial \tau_{\theta\theta}}{\partial \phi} = 0 \qquad (6\text{-}2\text{-}D)$$

$$\frac{\partial p}{\partial \phi} = 0 \qquad (6\text{-}2\text{-}E)$$

$$v_\phi = 0\,,\quad v_r = \rho g \cos\theta\,,\quad v_\theta = -\rho g \sin\theta \qquad (6\text{-}2\text{-}F)$$

Applying the assumptions in eqs. (6-2-B), (6-2-D), (6-2-E) and (6-2-F) to eq. (6-1), we obtain

$$\frac{1}{r}\frac{\tau_{\theta\phi}}{\partial\theta} + \frac{2}{r}\tau_{\theta\phi}\cot\theta = 0 \qquad (6\text{-}3)$$

The above equation can be rewritten as

$$\sin^2\theta \frac{\partial}{\partial\theta}\left(\tau_{\theta\phi}\sin^2\theta\right) = 0 \qquad (6\text{-}4)$$

which, on integration, gives

$$\tau_{\theta\phi}(\theta)\sin^2\theta = \text{constant}$$

Since $\sin\theta \neq 0$ for points in the gap; the constant

here must be independent of r and ϕ . $\mathcal{J}_{\theta\phi}$ is also independent of θ when $\Delta\theta$ is very small because it is a function of $\dot{r}$ alone*. The total torque M exerted by the fluid on the plate is given by

$$M = \int_0^R r\, \mathcal{J}_{\phi\theta}\left(\tfrac{\pi}{2}\right) d(\pi r^2) = \frac{2\pi}{3} R^3 \mathcal{J}_{\theta\phi}\left(\tfrac{\pi}{2}\right) \qquad (6\text{-}5)$$

where R is the radius of the plate. From eqs. (6-4) and (6-5) we obtain

$$\mathcal{J}_{\theta\phi} \doteq \frac{3M}{2\pi R^3} \qquad (6\text{-}6\text{-}A)$$

and

$$\eta = \frac{3M}{2\pi R^3 \dot{\gamma}} \qquad (6\text{-}6\text{-}B)$$

If the torsion bar constant k_t and the movement of torsion head transducer Δ_T are known we can express eqs. (6-6-A) and (6-6-B) as

$$\mathcal{J}_{\theta\phi} = \frac{3\,\Delta_T K_t}{2\pi R^3} \qquad (6\text{-}7\text{-}A)$$

$$\eta = \frac{3\Delta_T K_t}{2\pi R^3 \dot{\gamma}} \qquad (6\text{-}7\text{-}B)$$

---

* See eq. (6-2-C)

where R is the radius of platens (cm)

M is the torque

Δ_T is the movement of torsion head transducer in microns

K_t is the torsion bar constant in dynes-cm per micron movement of the transducer

(b) working equation of shear rates

From eq. (6-6-B), we know that η can be treated as a constant when $\Delta\theta$ becomes very small. We obtain the relationship between $\mathcal{J}_{\theta\phi}$ and the gradient of v_ϕ from the following equation (5)

$$\mathcal{J}_{\theta\phi} = -\eta \frac{\sin\theta}{r} - \frac{\partial}{\partial\theta}\left(\frac{v_\phi}{\sin\theta}\right) \tag{6-8}$$

When this equation is inserted into eq. (6-6-A), we get the following ordinary differential equation

$$\eta \sin\theta \frac{d}{d\theta}\left(\frac{v_\phi/r}{\sin\theta}\right) = \frac{3\,\mathcal{J}_{\theta\phi}}{2\pi R^3} \tag{6-9}$$

Based on the following conditions:

(i) $v_\phi = 0$ at $\theta = \frac{\pi}{2} + \Delta\theta$

(ii) $v_\phi = \Omega r$ at $\theta = \frac{\pi}{2}$

(iii) $\Delta\theta$ is very small

The solution of the above differential equation can be approximated by (5)

$$v_\phi = \frac{r\Lambda_0(\theta - \frac{\pi}{2})}{\Delta\theta} \tag{6-10}$$

The definition of $\dot{\gamma}$ is

$$\dot{\gamma} = \frac{\partial v_\phi}{r\partial\theta} \tag{6-11}$$

Therefore, by the use of eq. (6-10), we obtain

$$\dot{\gamma} = \frac{\frac{\Lambda_0}{\Delta\theta} r\partial\theta}{r\ \partial\theta} = \frac{\Lambda_0}{\Delta\theta} \tag{6-12}$$

(c) working equation of primary normal-stress differences

The r-component of the equation of motion in a spherical coordinate system has the following form

$$\rho\left(\frac{\partial v_r}{\partial t} + v_r\frac{\partial v_r}{\partial r} + \frac{v_\theta}{r}\frac{\partial v_r}{\partial\theta} + \frac{v_\phi}{r\sin\theta}\frac{\partial v_r}{\partial\phi} - \frac{v_\theta^2 + v_\phi^2}{r}\right)$$

$$= \frac{-\partial P}{\partial r} - \left[\frac{1}{r^2}\frac{\partial}{\partial r}(r^2\tau_{rr}) + \frac{1}{r\sin\theta}\frac{\partial}{\partial\theta}(\tau_{r\theta}\sin\theta)\right.$$

$$\left. + \frac{1}{r\sin\theta}\frac{\partial\tau_{r\phi}}{\partial\phi} - \frac{\tau_{\theta\theta} + \tau_{\phi\phi}}{r}\right] - \rho g\cos\theta \tag{6-13}$$

Based on the assumptions in eqs. (6-2-A), (6-2-B), (6-2-C), (6-2-D) and (6-2-F) (neglecting the centrifugal force term $-\rho v_\phi^2/r$) we get

$$0 = -\frac{1}{r^2}\frac{\partial}{\partial r}(r^2 \pi_{rr}) + \frac{-\tau_{\theta\theta} - \tau_{\phi\phi}}{r}$$

where $\pi_{rr} = P + \tau_{rr}$. A rearrangement gives

$$\frac{\partial \pi_{rr}}{\partial \ln r} = \pi_{\theta\theta} + \pi_{\phi\phi} - 2\pi_{rr} \qquad (6\text{-}14)$$

The above equation may be integrated from r = R to r = r to give

$$\pi_{\theta\theta} = \pi_{\theta\theta}(R) + (\pi_{\phi\phi} - \pi_{\theta\theta} - 2\pi_{rr}) \ln \frac{r}{R} \qquad (6\text{-}15)$$

where $\pi_{\phi\phi} - \pi_{\theta\theta} - 2\pi_{rr}$ is constant based on the fact that eq. (6-2-C) is valid. The total thrust of the fluid on the plate minus the thrust associated with atmospheric pressure P_a is

$$\mathcal{F}_1 = \int_A \pi_{\theta\theta}\, dA - \int_A P_a\, dA$$

$$= 2\pi \int_0^R \pi_{\theta\theta}\, r\, dr - \pi R^2 P_a \qquad (6\text{-}16)$$

Insertion of $\pi_{\theta\theta}$ from eq. (6-15) into (6-16) gives after integration

$$\mathcal{F}_1 = \pi R^2 \pi_{\theta\theta}(R) - \frac{1}{2}\pi R^2 (\pi_{\phi\phi} + \pi_{\theta\theta} - 2\pi_{rr}) - \pi r^2 P_a \qquad (6\text{-}17)$$

Then we make use of the fact that, if the free surface of the fluid is a spherical surface at r = R, $P_a = \pi_{rr}(R)$. Eq. (6-17) finally yields

$$\sigma_{\theta\theta} - \sigma_{\phi\phi} = \frac{2\mathcal{F}_1}{\pi R^2} \qquad (6\text{-}18\text{-}A)$$

From section (6-1) we know that the total thrust is the product of the reading of the micrometer and the rate of the leaf spring k_N. Therefore the working formula of primary normal-stress difference becomes

$$\sigma_{\theta\theta} - \sigma_{\phi\phi} = \frac{2\Delta_N k_N}{\pi R^2} \qquad (6\text{-}18\text{-}B)$$

where Δ_N is the reading or movement of micrometer in microns

k_N is the rate of the leaf spring in dynes per micron movement of the free end

(6.3) Presentation of Experimental Data and Model Evaluation

To gain insight into viscoelastic solution behavior three typical samples were tested. The first one used in this study is

(a) the polymer solution with 2% by weight polyisobutylene (PIB) in primol (a phamaceutical white oil). This solution was prepared by Dr. W. Philippoff and the experimental data by Dr. D. Huppler in University of Wisconsin. The cone angle used in the Weissenberg rheogoniometer is

$1^{o}37'$ with the plate diameter 7.5 cm.

The experimental data of this sample along with the predicted results from the Huang-Shangkuan (our) model are presented in Figs. 6-5 and 6-6. These results are also given in Table 6-1. The parameters estimated, by the use of the procedures given in section (5-10) for 2% PIB in primol, are : η_0 (9968), α_1 (5.56), λ_1 (90.5), α_2 (4.69), λ_2 (46.2), a(0.788), b(0.223), c(0.495), d(0.356). The results from the Spriggs and Bird-Carreau models are also given in the same figures (Figs. 6-5 and 6-6) for the purpose of comparison among these models.

As noted from these figures, the Spriggs model is found to have the following main weak points:

(i) The curve of log $-(\mathcal{J}_{11} - \mathcal{J}_{22})$ vs. log $\dot{\gamma}$ has, incorrectly, the same slope in the power-law region.

(ii) The slope of log $-(\mathcal{J}_{11} - \mathcal{J}_{22})$ vs. log $\dot{\gamma}$ is too rigidly related to the slope of the viscosity curve. In other words, only one parameter α is incorporated to predict the power-law behavior in both η and $-(\mathcal{J}_{11} - \mathcal{J}_{22})$ data. Therefore the difference between the predicted and the experimental data is significant. More experimental data along with the predicted results from the Spriggs model are given in Appendix 1 for the purpose of illustrating those discrepancies.

The Bird-Carreau model, developed later, has the capability to compensate for the above weak points. However,

Table 6-1

Tabulated Rheological Data for 2% Polyisobutylene in Primol

$\dot{r}$: a shear rate (sec)

η_{exp}: experimental non-Newtonian viscosities (poise)

η_{comp}: the viscosity from the Huang-Shangkuan model (poise)

$-(\tau_{11}-\tau_{22})_{exp}$: experimental primary normal-stress differences (dyne/cm^2)

$-(\tau_{11}-\tau_{22})_{comp}$: primary normal-stress differences from the Huang-Shangkuan model (dyne/cm^2)

Table 6-1

ν	η_{exp}	η_{comp}	$-(J_{11}-J_{22})_{exp}$	$-(J_{11}-J_{22})_{comp}$
5.27×10^{-2}	2.18×10^{3}	2.16×10^{3}	2.93×10^{2}	3.36×10^{2}
6.69×10^{-2}	1.93×10^{3}	1.82×10^{3}	3.30×10^{2}	3.78×10^{2}
8.39×10^{-2}	1.67×10^{3}	1.54×10^{3}	3.93×10^{2}	4.24×10^{2}
1.05×10^{-1}	1.42×10^{3}	1.32×10^{3}	5.35×10^{2}	4.76×10^{2}
1.33×10^{-1}	1.17×10^{3}	1.11×10^{3}	5.45×10^{2}	5.39×10^{2}
1.67×10^{-1}	1.01×10^{3}	9.59×10^{2}	6.20×10^{2}	6.09×10^{2}
2.11×10^{-1}	8.48×10^{2}	8.02×10^{2}	7.50×10^{2}	6.94×10^{2}
2.65×10^{-1}	7.51×10^{2}	6.88×10^{2}	7.50×10^{2}	7.90×10^{2}
3.33×10^{-1}	6.22×10^{2}	5.87×10^{2}	9.50×10^{2}	9.03×10^{2}
4.20×10^{-1}	5.19×10^{2}	5.00×10^{2}	1.14×10^{3}	1.04×10^{3}
5.27×10^{-1}	4.55×10^{2}	4.48×10^{2}	1.42×10^{3}	1.19×10^{3}
6.69×10^{-1}	3.72×10^{2}	3.69×10^{2}	1.47×10^{3}	1.39×10^{3}
8.39×10^{-1}	3.21×10^{2}	3.17×10^{2}	1.74×10^{3}	1.62×10^{3}
1.05	2.71×10^{2}	2.75×10^{2}	1.89×10^{3}	1.89×10^{3}
1.33	2.35×10^{2}	2.35×10^{2}	2.28×10^{3}	2.23×10^{3}
1.67	1.98×10^{2}	2.04×10^{2}	2.66×10^{3}	2.63×10^{3}
2.11	1.75×10^{2}	1.76×10^{2}	3.09×10^{3}	3.14×10^{3}
2.66	1.48×10^{2}	1.54×10^{2}	3.75×10^{3}	3.77×10^{3}
3.33	1.29×10^{2}	1.34×10^{2}	4.50×10^{3}	4.54×10^{3}
4.20	1.15×10^{2}	1.17×10^{2}	5.40×10^{3}	5.53×10^{3}
5.27	9.45×10^{1}	1.03×10^{2}	6.60×10^{3}	6.67×10^{3}
6.69	8.86×10^{1}	9.01×10^{1}	8.40×10^{3}	8.46×10^{3}
8.39	7.66×10^{1}	7.97×10^{1}	1.06×10^{4}	1.05×10^{4}
1.05×10^{1}	7.07×10^{1}	7.07×10^{1}	1.35×10^{4}	1.33×10^{4}
1.33×10^{1}	6.35×10^{1}	6.27×10^{1}	1.74×10^{4}	1.70×10^{4}
1.67×10^{1}	5.81×10^{1}	5.60×10^{1}	2.27×10^{4}	2.20×10^{4}
2.11×10^{1}	5.12×10^{1}	5.00×10^{1}	3.04×10^{4}	2.90×10^{4}
2.66×10^{1}	4.67×10^{1}	4.50×10^{1}	3.86×10^{4}	3.85×10^{4}
3.33×10^{1}	4.25×10^{1}	4.07×10^{1}	5.30×10^{4}	5.17×10^{4}

Fig. 6-5

Non-Newtonian Viscosities for 2% Polyisobutylene (PIB)

Data of Dr Huppler (55)

△ △ △ Experimental data from the Weissenberg Rheogoniometer

—··—·· The Spriggs model (13)

the parameters are η_0 : 11500 poise
α : 3.5
λ : 145 sec
c : 0.39

— — — The Bird-Carreau model (13)

the parameters are η_0 : 9968 poise
α_1 : 2.85
α_2 : 2.33
λ_1 : 149.5 sec
λ_2 : 170.3 sec

——— The Huang-Shangkuan model

the parameters are η_0 : 9968 poise
α_1 : 5.56
α_2 : 4.69
λ_1 : 90.5 sec
λ_2 : 46.2 sec
a : 0.788
b : 0.223
c : 0.495
d : 0.356

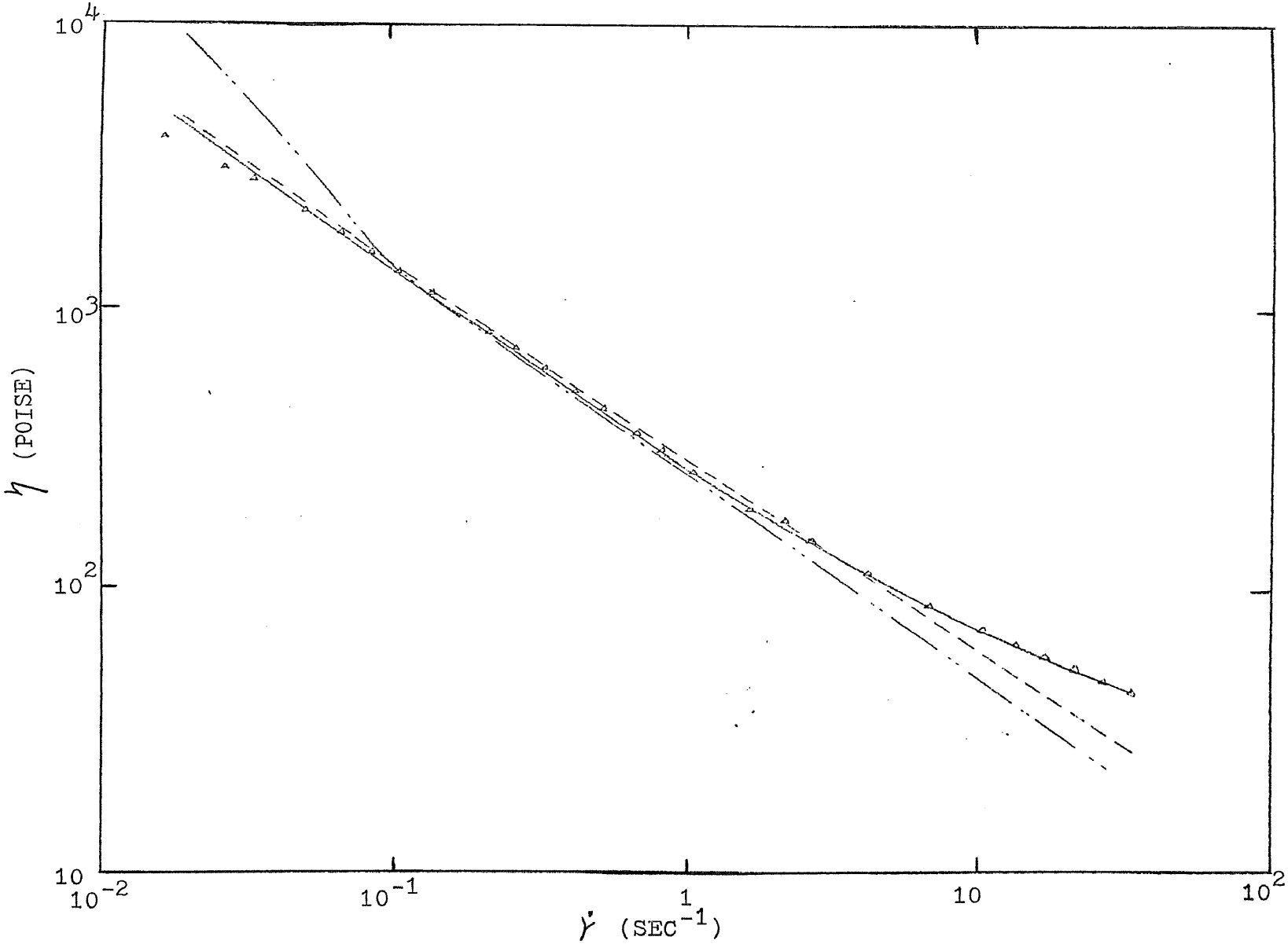
10^4
10^3
10^2
10
η (POISE)
10^{-2}
10^{-1}
1
10
10^2
$\dot{\gamma}$ (SEC^{-1})

Fig. 6-6

Normal-Stress Difference for 2% Polyisobutylene (PIB).
Data of Dr. Huppler (55)

△ △ △ Experimental data from the Weissenberg Rheogoniometer

— ·· — ·· The Spriggs model (13)

the parameters are η_0 : 11500 poise
α : 3.5
λ : 145 sec
C : 0.39

— — — The Bird-Carreau model (13)

the parameters are η_0 : 9968 poise
α_1 : 2.85
α_2 : 2.33
λ_1 : 149.5 sec
λ_2 : 170.3 sec

———— The Huang-Shangkuan model

the parameters are η_0 : 9968 poise
α_1 : 5.56
α_2 : 4.69
λ_1 : 90.5 sec
λ_2 : 46.2 sec
a : 0.788
b : 4.47
c : 0.495
d : 2.81

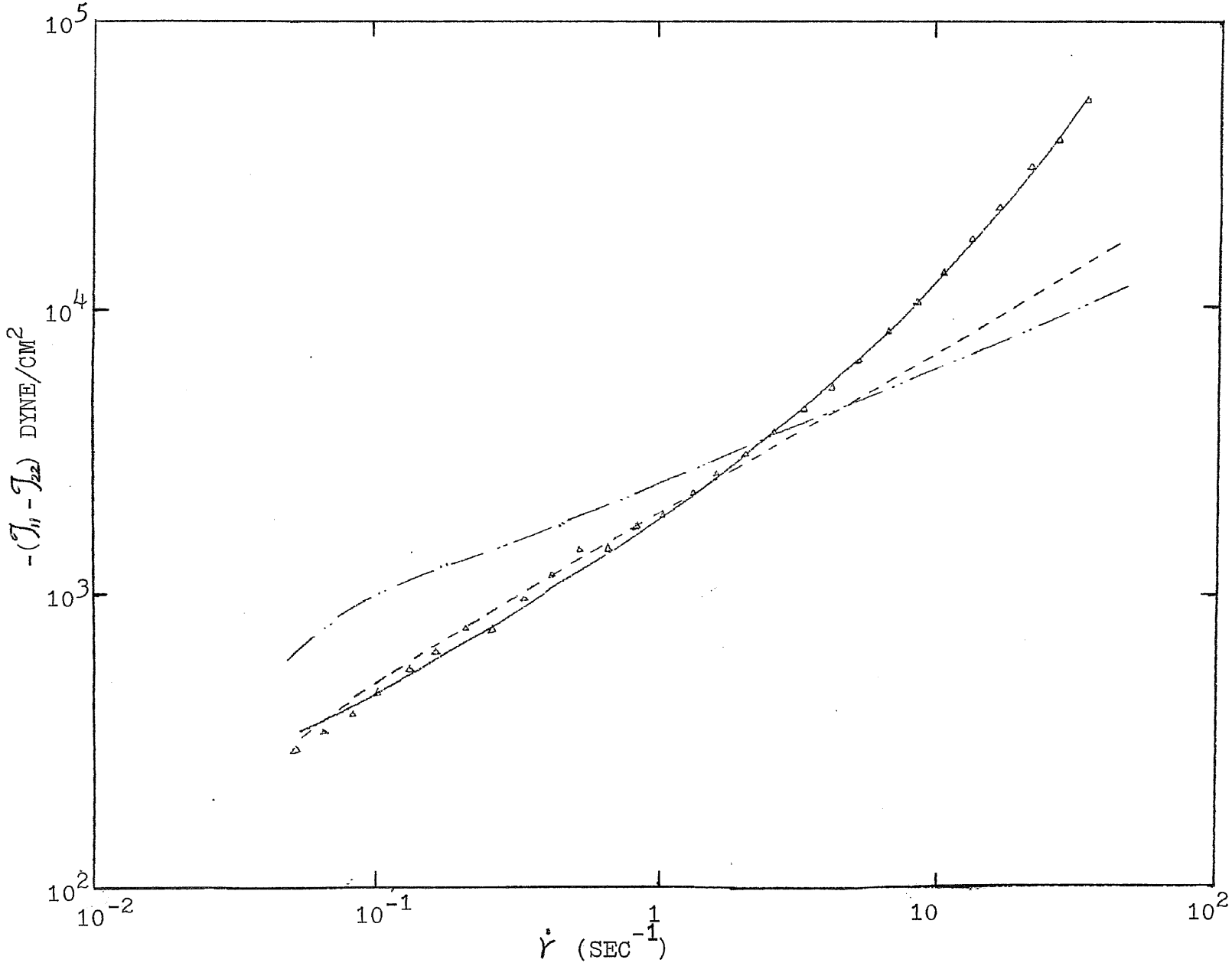
10^5
10^4
10^3
10^2
$-(\mathcal{T}_{11} - \mathcal{T}_{22})$ DYNE/CM^2
10^{-2}
10^{-1}
1
10
10^2
$\dot{\gamma}$ (SEC^{-1})

discrepancies at high shear rates in the Bird-Carreau model have been obviously observed; the power-law behavior in region III extends directly to region IV at high shear rates.

Contrary to the unsatisfactory predictions by the Bird-Carreau and Spriggs models, a good agreement between the experimental data and the Huang-Shangkuan model is observed from Figs. 6-5 and 6-6. One comes to the conclusion that, if parameters a and c in eqs. (5-46) and (5-47) are

(i) larger than 0, the Huang-Shangkuan model describes exactly region IV behavior of polymer solutions; in this case, 2% PIB solution is a typical example.

(ii) equal to 0, the Huang-Shangkuan model describes the power-law behavior. In this case, the Huang-Shangkuan model can be reduced to the Bird-Carreau model. Therefore we can regard the Bird-Carreau model as a special case of the Huang-Shangkuan model.

(b) The experimental data of two polymer solutions were taken in our laboratory and evaluated using the Huang-Shangkuan model in order to illustrate the condition (ii) mentioned above. The results are given in Figs. 6-7 and 6-8. The cone angle $1^{o}58'$ with the plate diameter 5 cm are used in the Weissenberg rheogoniometer.

The discussions above reveal that the Huang-Shangkuan model has a better agreement than the other two models when these typical samples were tested. We also include in Appendix 1 some other important constitutive equations or

rheological models proposed in recent years, such as the Tanner-Simmons model, the Nakamura-Yoshika rigid-chain model, etc. to illustrate the inadequacy in their predictions of the viscosity and normal stress data. Rather intensive review of these models has been given by Spriggs and Carreau (14)(43).

Fig. 6-7

Non-Newtonian Viscosities and Normal-Stress Differences for 2% MD-333 in Primol 355.

△ △ △ △ △ △ : Experimental data of viscosity

▲ ▲ ▲ ▲ ▲ ▲ : Experimental data of normal-stress difference

——————— : Evalution of the Huang-Shangkuan model the parameters are

η_0 : 51 poise

α_1 : 1.398

α_2 : 0.6589

λ_1 : 0.3263 sec

λ_2 : 0.5317 sec

a : 0

b : arbitrary constant

c : 0

d : arbitrary constant

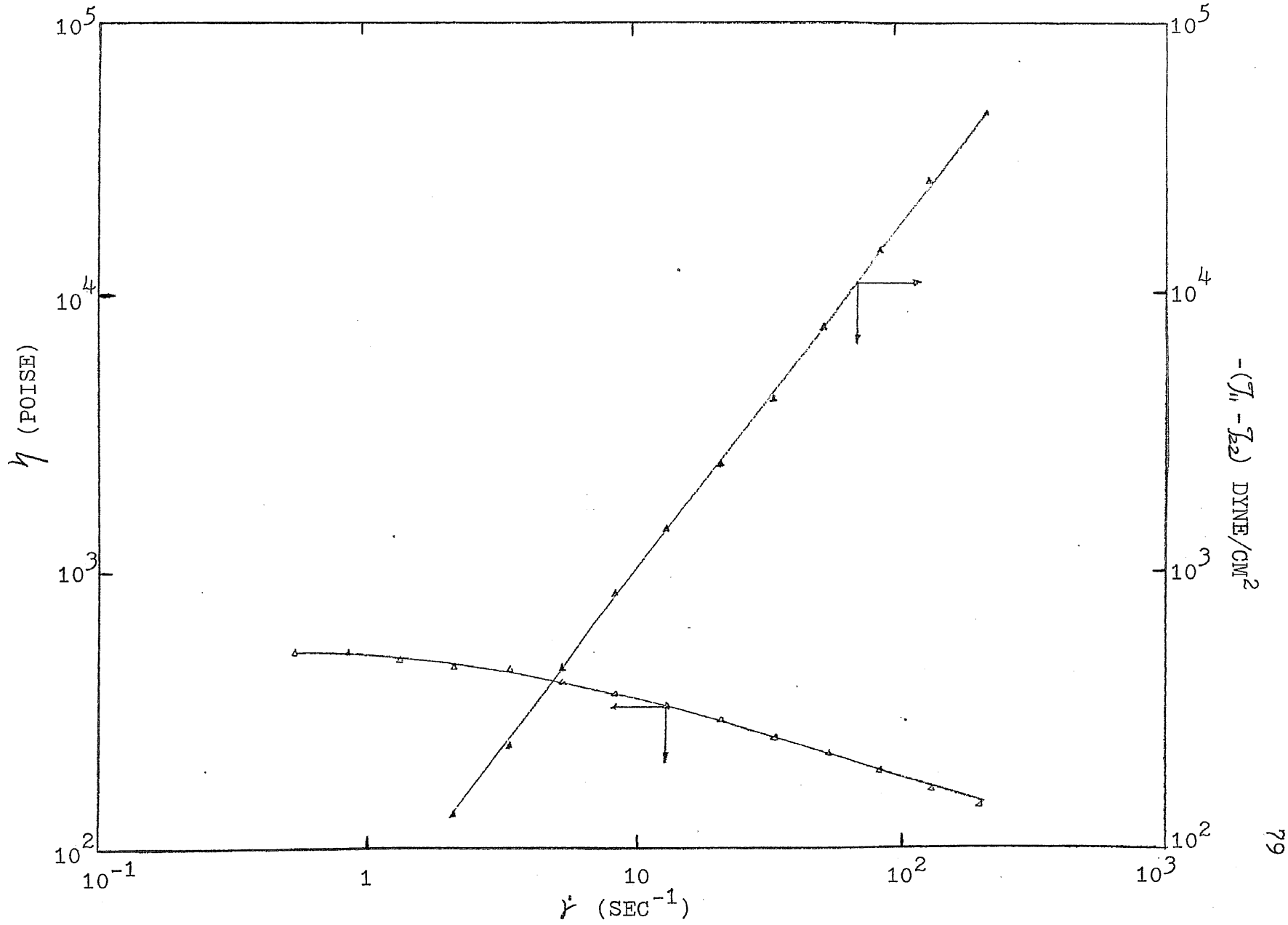
10^5
10^4
10^3
10^2
η (POISE)
10^{-1}
1
10
10^2
10^3
$\dot{\gamma}$ (SEC^{-1})
$-(\mathcal{T}_{11} - \mathcal{T}_{22})$ DYNE/CM^2

Fig. 6-8

Non-Newtonian Viscosities and Normal-Stress Differences for Polystyrene S-111 15% in Aroclor-1248 "denatured"

△ △ △ △ : Experimental data of viscosity

▲ ▲ ▲ ▲ : Experimental data of normal-stress difference

———— : Evaluation of the Huang-Shangkuan model tha parameters are

η_0 : 6700 poise

α_1 : 1.8416

α_2 : 0.3803

λ_1 : 0.272

λ_2 : 0.2285

a : 0

b : arbitrary constant

c : 0

d : arbitrary constant

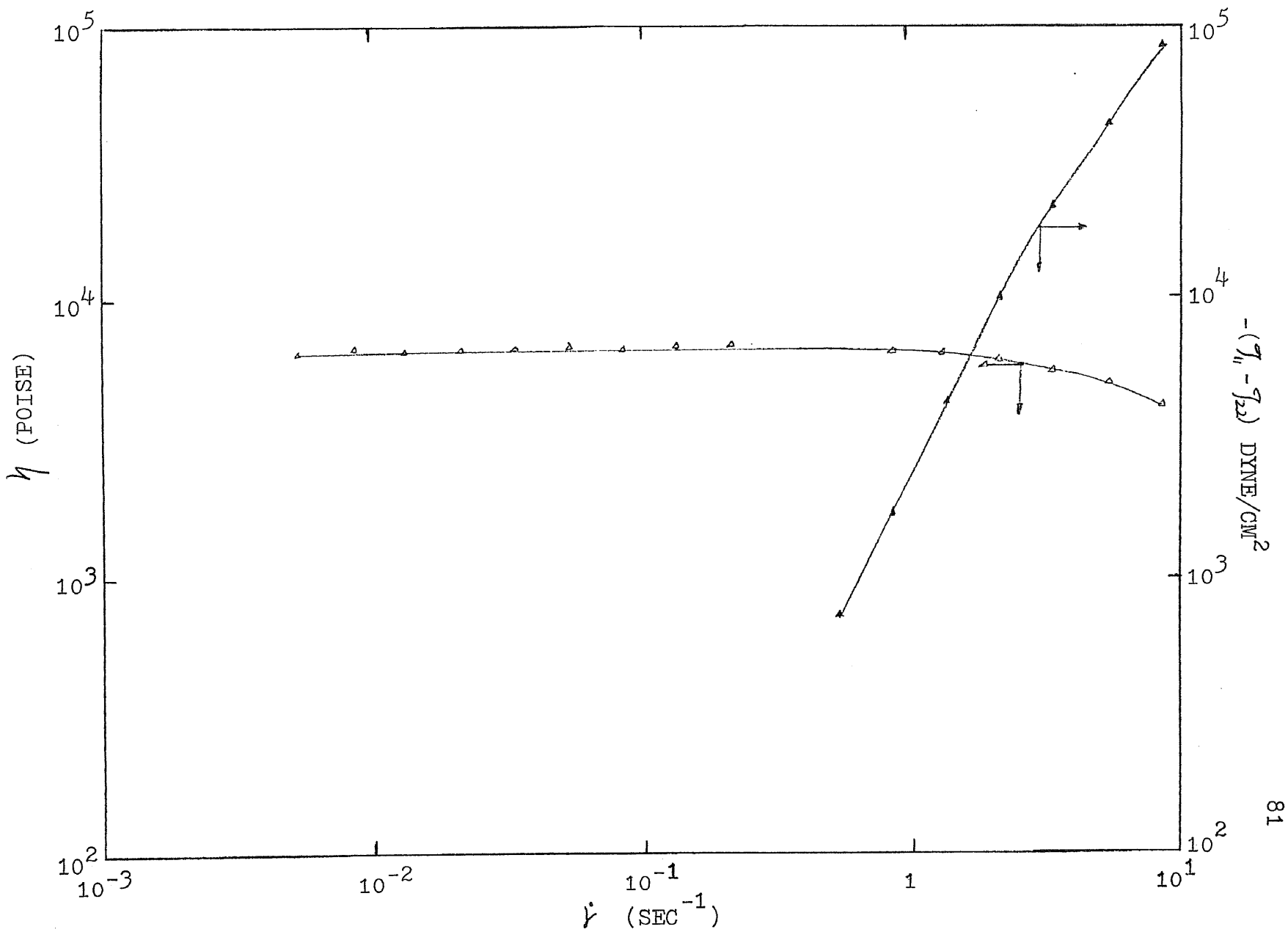
10^5
10^4
10^3
10^2
η (POISE)
10^{-3}
10^{-2}
10^{-1}
1
10^1
$\dot{\gamma}$ (SEC^{-1})
10^5
10^4
10^3
10^2
$-(\tau_{11} - \tau_{22})$ DYNE/CM^2

CHAPTER 7 CONCLUSIONS AND RECOMMENDATIONS

The principal objective of this dissertation is to propose a realistic rheological model in conjunction with Rouse's theory and Lodge's network theory. The Huang-Shangkuan model has three important aspects:

(a) It has been demonstrated that our model gives the best representation of the experimental data for a wide range of shear rates in comparison with the Spriggs model and the Bird-Carreau model.

(b) In the high shear rate region (region IV) the Huang-Shangkuan model is distinguished among other models by its capability to predict the shear stress and the primary normal stress difference which the other models fail to predict.

(c) Our approach to nonlinear viscoelastic model building is original in that we postulate that the time constant and the viscosity parameters are dependent on the second rate-of-strain invariant.

In summary, the following areas are considered in developing and testing the Huang-Shangkuan model:

Continuum mechanics provides the mathematical framework (kinematic definitions, tensor equations, etc.) for expressing a specific relation between the stresses and kinematic variables.

Lodge's network theory has provided some specific information in explaining molecular behavior such as the creation and

the loss of network junctions in polymer solutions. Rouse's theory has provided the starting point in reducing an unlimited number of parameters in the Huang-Shangkuan model. Primary experiments, including the measurement of normal stress differences and viscosities, provide the necessary tests for our model.

RECOMMENDATIONS

There are a number of interesting studies which merit consideration:

(a) Develop some successful rheological models for concentrated polymer solutions entirely from the molecular point of view. Although some molecular theories such as bead-spring theories, chain-chain interaction theories or network theories, have been developed in recent years, they are not quite successful in predicting rheological preperties of high polymers. A sound molecular theory would help in properly relating model parameters to physical properties such as molecular weight, chain branching, chain stiffness, temperature and other important variables of high polymers.

(b) There is a lot of controversy concerning the magnitude, sign and shear rate dependence of the second normal stress difference $-(\mathcal{J}_{22} - \mathcal{J}_{33})$. Accurate measurement and theoretical study of this stress would permit us to understand the relation between $-(\mathcal{J}_{11} - \mathcal{J}_{22})$ and $-(\mathcal{J}_{22} - \mathcal{J}_{33})$.

(c) For extremely difficult flow problems where the prospects of getting an analytical solution seem hopeless, dimensionless analysis may be possible. In our model, the parameters η_0 , α_1 , α_2 , λ_1 , λ_2, a, b, c and d can be used to construct dimensionless groups. These groups may then be employed to get data correlations. Due to the fact that complicated behavior exists in polymer solutions, such correlations will require an enormous amount of effort to derive.

NOMENCLATURE

a,b,c,d	dimensionless parameters related to experimental observations at high shear rate in region IV
$\underline{\underline{C}}(t,t_0)$	Cauchy tensor
$\underline{\underline{C}}^{-1}(t,t_0)$	Finger tensor
$\underline{\underline{C}}(t_0,t)$	Green tensor
$\underline{\underline{C}}^{-1}(t_0,t)$	Piola tensor
	Jaumann derivative
$\underline{\underline{e}}$	rate of deformation tensor
	the total thrust of the fluid on the plate in a cone-and-plate viscometer
$\underline{\underline{F}},\underline{\underline{F}}^{-1}$	displacement tensors
$\underline{\underline{F}}^{T}$	the transpose of $\underline{\underline{F}}$
$\underline{\underline{F}}^{-1T}$	The transpose of $\underline{\underline{F}}^{-1}$
	a functional of t' throughout the interval $t_0 \leqslant t' \leqslant t$
g_i	covariant base vector in a fixed coordinate system
g^{ij}	contravariant metric tensor in a fixed coordinate system
$\hat{\underline{g}}_{\alpha}(\xi t)$	convected covariant base vector
$\hat{\underline{g}}^{\alpha}(\xi t)$	convected contravariant base vector
k	Botzmann's constant
k_n	the rate of the movement of the leaf spring in the Weissenberg rheogoniometer
k_t	torsion bar constant
K_i	the kernel of i-th integral of a functional
L_2	second rate-of-strain invariant
M	the torque exerted by the fluid on the torsion bar

n_1, n_2	two constants in the Bird-Carreau model
$N(t-t')$	the junction age distribution function
R	the radius of the plate in a cone-and-plate viscometer
SUM	an objective function defined as $\sum_{i=1}^{\infty}((Y_i-\hat{Y}_i)/\hat{Y}_i)^2$
$\bar{V}V$	dyadic product of gradient $\bar{V}$ and velocity V
X^i	fixed coordinate system
$\hat{Y}_i$	experimental or observed points
Y_i	computed points from the Huang-Shangkuan model
T	movement of torsion head transducer in microns
N	reading or movement of micrometer
Ω_0	angular velocity
ξ^i	convected coordinate system
τ_{xy} (τ_{ij})	shear stress on the xz(ik) plane vertical to y(j) axis
$-(\tau_{11}-\tau_{zz})$	primary normal stress difference
$-(\tau_{\theta\theta}-\tau_{\phi\phi})$	primary normal stress difference in a cone-and-plate system
μ	Newtonian viscosity
η_0	zero-shear-rate viscosity
η	non-Newtonian viscosity
η_p	viscosity of p-th segment in a polymer chain
λ_s, η_s	functions of the second rate-of-strain invariant in the Huang-Shangkuan model
λ_{1p}	the time constant of p-th segment of a polymer chain associated with the rate of creation of network junctions
λ_{2p}	the time constant of p-th segment of a polymer chain associated with the rate of loss of network junctions

$\dot{\gamma}$	the magnitude of $\dot{\gamma}_{yx}$ at steady-state shearing flow
$\dot{\gamma}_{yx}$	infinitesimal rate of strain tensor
λ_1, λ_2	time constants associated with λ_{1p} , λ_{2p}
α_1, α_2	dimensionless parameters associated with the slope in the power law region
δ_j^i	Kronecker delta
Γ_j^i	finite strain tensor
μ_1, μ_2, μ_3	unspecified memory functions in Coleman and Noll's functional analysis
δ	primary normal-stress-difference coefficient
β	second normal-stress-difference coefficient

REFERENCES

1. Bauer W. H., and Collins E. A., Rheology. New York: Acamedic Press, 1967, p. 423-459.

2. Berstein B., Kearsley E. A., and Zapas L. J., Trans. Soc. Rheol., 9, 1965, p. 27.

3. Berstein B., Kearsley E. A., and Zapas L. J., Trans. Soc. Rheol., 68B, 1964, p. 103.

4. Berstein B., Kearsley E. A., and Zapas L. J., Trans. Soc. Rheol., 7, 1963, p. 391

5. Bird R. B., Stewart W., and Lightfoot E., Transport Phenomena. New York: John Wiley and Sons, 1960, p. 5.

6. Bird R. B., and Carreau P. J., Chem. Eng. Sci., 23, 1968, p. 427-434.

7. Bird R. B., "Notes on Macromolecular Hydrodynamics", AIChE Continuing Education Series, 4, 1968, p. 1-15.

8. Bogue D. C., I. E. C. Fund., 5, 1966, p. 253.

9. Bogue D. C., and Doughty J. O., I. E. C. Fund., 5, 1966, p. 243.

10. Brydson J. A., Flow Properties of Polymer Melts. Van Nostrand Reinhold Co., 1970, p. 7-20.

11. Burow S. P., Peterlin S. A., and Turner D. T., Polymer, 6, 1965, p. 35-37.

12. Carreau P. J., McDonald I. F., and Bird R. B., Chem. Eng. Sci., 23, 1968, p. 901-910.

13. Carreau P. J., Trans. Soc. Rheol., 16:1, 1972, p. 99-127.

14. Carreau P. J., Ph. D. Thesis, University of Wisconsin, 1968, p. 3.

15. Coleman B. D., and Noll W., Rev. Mod. Phys., 33, 1961, p. 239. Erratum, 36, 1964, p. 1103.

16. Coleman B. D., Markovitz H., and Noll W., Viscometric Flows of Non-Newtonian Fluids. New York: Springer, 1966.

17. Doughty J. O., and Bougue D. C., I. E. C. Fund., 6, 1967, p. 388

18. Eringen A. C., Nonlinear Theory of Continuous Media. New York: McGraw Hill, 1962.

19. Ferry J. D., Viscoelastic Properties of Polymers. Chap. 1 and 2, New York: John Wiley and Sons, 1961.

20. Fixman M. J., J. Chem. Phys., 42, 1965, p. 3831-3837.

21. Fredrickson A. G., Principles and Applications of Rheology. New Jersey: Prentice-Hall, 1964.

22. Fredrickson A. G., Chem. Eng. Sci., 17, 1962, p. 155-166.

23. Green A. E., and Rivlin R. S., Arch. Rat. Mech. Anal. 1, 1957, p. 1.

24. Han C. D., Kim K. U., Siskovic N., and Huang C. R., unpublished preliminary report " An Appraisal of Rheological Models as Applied to Polymer Melt Flow", 1973.

25. Huppler J. D., Ashare E., and Holmes L. A., Trans. Soc. Rheol., 11:2, 1967, p. 159.

26. Huppler J. D., "Experimental Data for 2% PIB in Primol", University of Wisconsin, 1966.

27. Huppler J. D., McDonald I. F., Ashare E., Spriggs T. W., and Bird R. B., Trans. Soc. Rheol., 11:2, 1967 p. 181.

28. Huppler J. D., Trans. Soc. Rheol., 9:2, 1965, p. 273-286.

29. Lodge A. S., Elastic Liquids. New York: Academic Press, 1964.

30. Marquardt D. W., "Least-Square Estimation of Nonlinear Parameters", Engineering Department, E. I. DuPont De Nemours & Co., Inc., 1964.

31. Mckelvey J. M., Polymer Processing. New York: John Wiley and Sons, 1962.

32. Middleman S., The Flow of High Polymers. Interscience Publishers, 1968, p. 200-220.

33. Noll W. J., Rat. Mech. Anal., 4, 1955, p. 3-81.

34. Oldroyd J. G., Second Order Effects in Elasticity, Plasticity and Fluid Mechanics. New York: McMillian, 1964.

35. Oldroyd J. G., Proc. Roy. Soc., (London), A245, 1958, p. 278-297.

36. Oldroyd J. G., Proc. Roy. Soc., A2000, 1950, p. 523.

37. Ralston A., A First Course in Numerical Analysis. New York: McGraw-Hill, 1965, p. 131-136.

38. Roscoe R., Brit. J. Applied Phys., 15, 1964, p. 1095.

39. Rouse P. E., J. Chem. Phys., 21, 1953, p. 1272.

40. Sedov L. I., Introduction to the Mechanics of a Continuous Medium. Addison-Wesley, 1965.

41. Spiegel M. R., "Theory and Problems of Vector Analysis", Schaum's Outline Series, 1959, p. 147.

42. Spriggs T. W., Huppler J. D., and Bird R. B., Trans. Soc. Rheol., 10:1, 1966, p. 191.

43. Spriggs T. W., Ph. D. Thesis, University of Wisconsin, 1966.

44. Spriggs T. W., Chem. Eng. Sci., 20, 1965, p. 931-940.

45. Treloar L. R. G., The Physics of Rubber Elasticity. 2nd Edition, Clarendon Press, Oxford.

46. Volterra V., and Peres J., "Theorie Generale des Fonctionelles", Gauthier-Villars, Paris, 1, 1936, p. 61.

47. Walters K., Quant. J. Mech. Appl. Math., 13, 1960, p. 444; 15, 1962, p. 63.

48. White J. L., and Metzner A. B., J. Polymer Sci., 7, 1963, 0. 1867.

49. Wilde D. J., and Beighter C. S., Foundations of Optimization. Prentice-Hall, Inc., 1967.

50. Wilkinson W. L., Non-Newtonian Fluids. Pergamon Press, 1960, p. 10-17.

51. Williams M. C., AIChE J., 12, 1966, p. 1064-1070; 13, 1967, p. 534-537; 13, 1967, p. 955-961.

52. Wills A. F., Vector Analysis with an Introduction to Tensor Analysis. Dover, 1958.

53. Yamamoto M., J. Phys. Soc., (Japan), 11, 1956, p. 413; 12, 1957, p. 1148; 13, 1958, p. 1200.

54. Zimm B. H., J. Chem. Phys., 24, 1956, p. 269-278.

APPENDIX 1

Rheological Data with the Predicted Results from the Bogue Model, the Spriggs Model, the Tanner-Simmons Model, the Bird-Carreau Model and the Nakamura-Yoshika Rigid-Chain Model

Fig. A-1

Non-Newtonian viscosity and primary normal stress difference for 4% polystyrene, PS-4.0-1800-48 (28)

———————— the Bogue model

– – – – – – – – – the Spriggs model

—··—··—··—·· the Tanner-Simmons model

△ △ △ △ △ △ △ △ experimental data of viscosity

▲ ▲ ▲ ▲ ▲ ▲ ▲ experimental data of normal stress difference

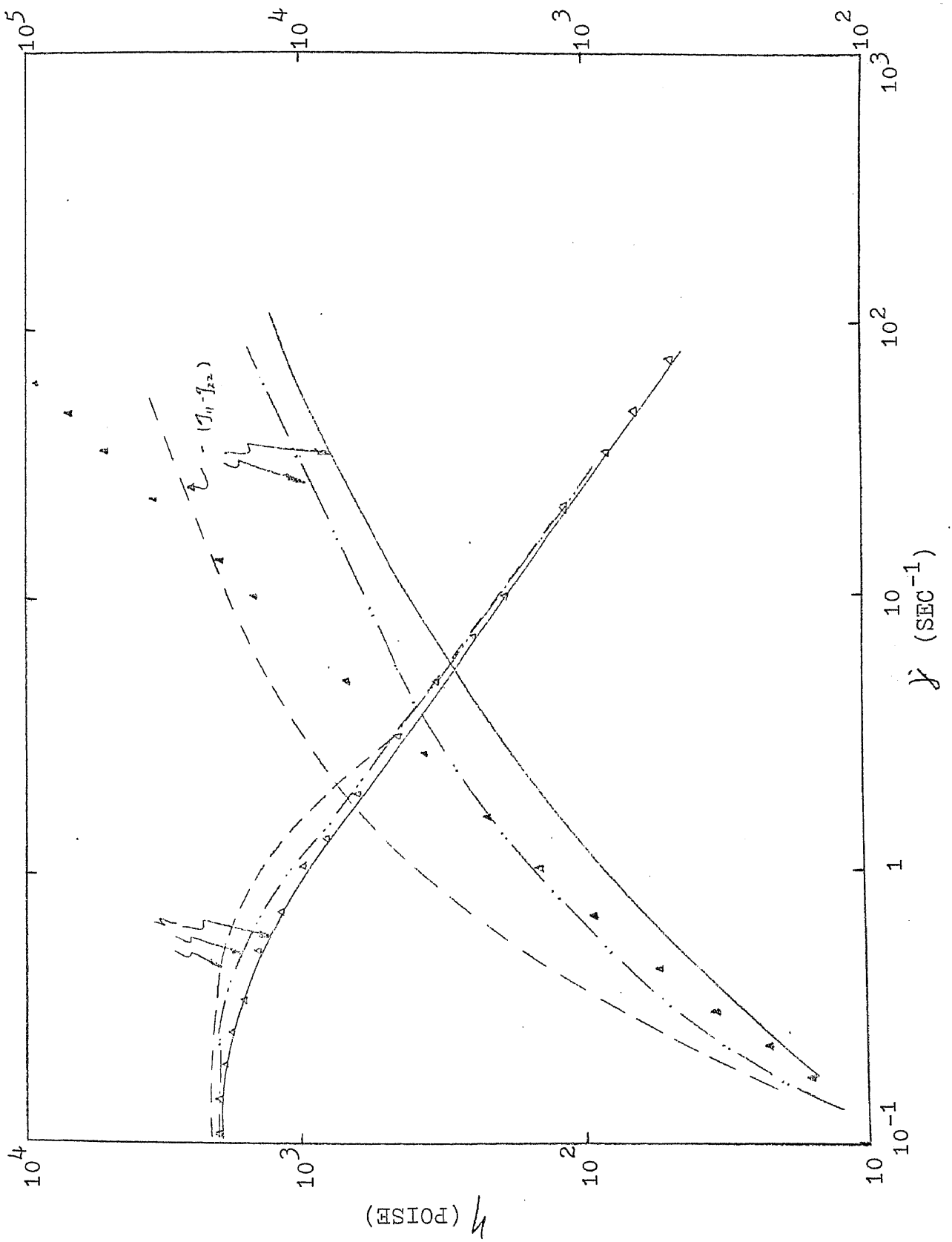
$-(\mathcal{T}_{11} - \mathcal{T}_{22})$ DYNE/CM^2
10^5
10^4
10^3
10^2
η (POISE)
10^4
10^3
10^2
10
10^{-1}
$\dot{\gamma}$ (SEC^{-1})
τ
$\tau - (\mathcal{T}_{11} - \mathcal{T}_{22})$
η

Fig. A-2

Non-Newtonian viscosity and normal stress differnece for 1.5% polyacrylamide (SEPARAN-30) (28)

the Bird-Carreau model

the Nakamura-Yoshika rigid chain model

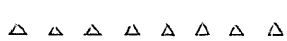
experimental data of viscosity


experimental data of normal stress difference

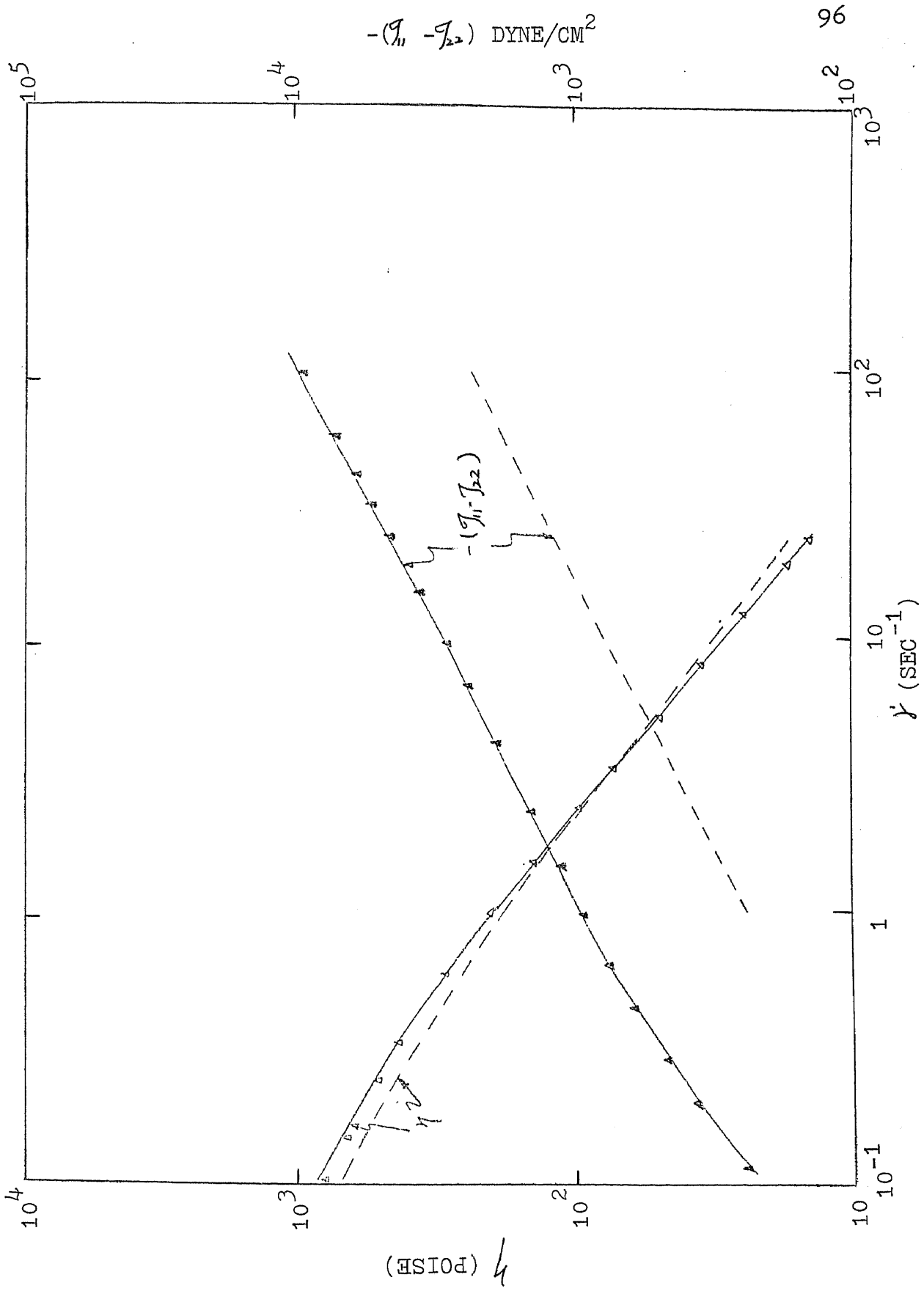
$-(\mathcal{T}_{11} - \mathcal{T}_{22})$ DYNE/CM^2
10^5
10^4
10^3
10^2
10^4
10^3
10^2
10^3
10^2
10
1
10^{-1}
$\dot{\gamma}$ (SEC^{-1})
$-(\mathcal{T}_{11}-\mathcal{T}_{22})$
η
η (POISE)

APPENDIX 2

The Computer Program in Search of Optimal Parameters in the Huang-Shangkuan Model

```
C       PROGRAM MAIN
        DIMENSION GAMMA(100),EP12(100),P12(100),EP1122(100),
       1EB2(100),B2(100),C2(100),D4(100),EC3(100),zeta(100),
       2EZETA(100),C3(100)
CC
C       INCORPORATE ZERO VISCOSITY ZETA0
        ZETA0=9968.
        NA=29
CC
C       READ IN SHEAR RATE AND EXPERIMENTAL DATA OF SHEAR
C       STRESS AND NORMAL-STRESS DIFFERENCE
        READ(5,1) (GAMMA(I),I=1,NA)
      1 FORMAT(8F10.4/8F10.4/8F10.4/8F10.4)
        READ(5,1) (EP12(I),I=1,NA)
        READ(5,1) (EP1122(I),I=1,NA)
        DO 20 I=1,NA
CC
C       CALCULATE NON-NEWTONIAN VISCOSITY
C       INCORPORATE PARAMETERS R,S,M,N WHERE LOGR=A, 1/S=B,
C       LOGM=C, 1/N=D
     20 EZETA(I)=EP12(I)/GAMMA(I)
        R=2.2
        S=4.47
        XM=1.64
        XN=2.81
        DO 2 I=1,NA
        C2(I)=R**(GAMMA(I)**(1./S))
        EB2(I)=EP12(I)/C2(I)
        D4(I)=XM**(GAMMA(I)**(1./XN))
        EC3(I)=EP1122(I)/(C2(I)*D4(I))
        WRITE(6,11)GAMMA(I),R,S,C2(I)
     11 FORMAT(1X,'........','GAMMA,R,S,C2',4(2X,E15.6)/)
      2 WRITE(6,4)XM,XN,D4(I)
      4 FORMAT(1X,'*********','XM,XN,D4',3(2X,E15.6)/)
        AMDA1=85.5
```

```
      AMDA2=39.2
      DO 3 M=1,10
CC
C     START TO SEARCH BEST SETS OF PARAMETERS AMDA1, AMDA2,
C     ALPHA1, ALPHA2
      AMDA1=AMDA1+1.0
      ALPHA1=5.06
      DO 3 N=1,10
      ALPHA1=ALPHA1+1.0
      SUMB2=0.
C     SUMB2, SUMP12, SUMZE ARE OBJECTIVE FUNCTIONS
      SUMP12=0.
      SUMZE=0.
      DO 3 I=1,NA
      B2(I)=ZETA0/(Z(ALPHA1)-1.)*3.1416*(2.**(ALPHA1)*AMDA1
     1*GAMMA(I))**((1.-ALPHA1)/ALPHA1)/(2.*ALPHA1*SIN(1.+
     2ALPHA1)/(2.*ALPHA1)*3.1416))*GAMMA(I)
      SUMB2=SUMB2+((B2(I)-EB2(I))/EB2(I))**2
      WRITE(6,5)AMDA1,ALPHA1,GAMMA(I),EB2(I),B2(I),SUMB2
    5 FORMAT(1X,'AMDA1,ALPHA1,GAMMA,EB2,B2,SUMB2',6(1X,E14.5)/)
      P12(I)=B2(I)*C2(I)
      ZETA(I)=P12(I)/GAMMA(I)
      SUMP12=SUMP12+((P12(I)-EP12(I))/EP12(I))**2
      SUMZE=SUMZE+((ZETA(I)-EZETA(I))/EZETA(I))**2
      WRITE(6,7)GAMMA(I),EP12(I),P12(I),SUMP12
    7 FORMAT(1X,'GAMMA,EP12,P12,SUMP12',4(2X,E15.6)/)
      WRITE(6,8)EZETA(I),ZETA(I),SUMZE
    8 FORMAT(1X,'EZETA,ZETA,SUMZE',3(2X,E15.6)/)
    3 CONTINUE
      AMDA1=90.5
      ALPHA1=5.56
      AMDA2=40.2
      DO 21 M=1,10
      AMDA2=AMDA2+1.0
      ALPHA2=4.29
```

```
      DO 21 N=1,10
      ALPHA2=ALPHA2+0.1
      WRITE(6,12) AMDA2,ALPHA2,AMDA1,ALPHA1,XM,XN
   12 FORMAT(1X,'AMDA2,ALPHA2,AMDA1,ALPHA1,XM,XN',6(1X,F10.4)/)
      SUMC3=0.
      SUMPN=0.
      DO 21 I=1,NA
      C3(I)=ZETA0*2.**(ALPHA2+1.0)*AMDA2/(Z(ALPHA1)-1.0)*
     13.1416*(2.**ALPHA1*AMDA1*GAMMA(I))**((1.-ALPHA1-ALPHA2
     2)/ALPHA1)/(2.*ALPHA1*SIN((1.+ALPHA1-ALPHA2)/(2.*ALPHA1)
     3*3.1416))*GAMMA(I)**2
      SUMC3=SUMC3+((C3(I)-EC3(I))/EC3(I))**2
      P1122(I)=C2(I)*C3(I)*D4(I)
      SUMPN=SUMPN+((P1122(I)-EP1122(I))/EP1122(I))**2
      WRITE(6,26)GAMMA(I),EP1122(I),P1122(I),SUMPN
   26 FORMAT(1X,'GAMMA,EP1122,P1122,SUMPN',4(2X,E15.6))
   21 WRITE(6,22)GAMMA(I),EC3(I),C3(I),SUMC3
   22 FORMAT(1X,'GAMMA,EC3,C3,SUMC3',4(1X,E15.6)/)
      STOP
      END


      FUNCTION Z(X)
C     THIS IS A RIEMANN ZETA FUNCTION SUBROUTINE
      Z=1.
      T=-X
      E2=EXP(T*0.6931471806)
      E3=EXP(T*1.0986122887)
      E4=E2*E2
      Z=Z+E2+E3+E4+EXP(T*1.60943791240)+E2*E2+EXP(T*1.9459101490
     1)+E2*E4*(0.5+8./(X-1.)+X*0.01041667*(1.0-0.000260417*
     2(X+1.)*(X+2.)*(1.0-0.000372*(X+3)*(X+4))))
      RETURN
      END
```